DESIGN, CONSTRUCTION, AND TESTING OF A COMPACT USB POWERED POTENTIOSTAT FOR BIOSENSOR APPLICATIONS

by

Carlyn Loncaric
B.A.Sc., Simon Fraser University 2009

THESIS SUBMITTED IN PARTIAL FULFILLMENT OF
THE REQUIREMENTS FOR THE DEGREE OF

MASTER OF APPLIED SCIENCE

In the
School of Engineering Science

SIMON FRASER UNIVERSITY

Spring 2011

APPROVAL

Name: **Carlyn Loncaric**

Degree: **Master of Applied Science**

Title of Thesis: **Design, construction, and testing of a compact USB powered potentiostat for biosensor applications**

Examining Committee:

Chair: **Michael Sjoerdsma, Lecturer**
School of Engineering Science

_____

Dr. Ash M. Parameswaran, P. Eng
Senior Supervisor
Professor, School of Engineering Science

_____

Dr. Hua-Zhong Yu
Supervisor
Professor, Department of Chemistry

_____

Dr. Marinko Sarunic, P. Eng
Internal Examiner
Assistant Professor, School of Engineering Science

Date Defended/Approved: 20 April 2011

Declaration of
Partial Copyright Licence

ABSTRACT

This thesis investigates the design, construction and testing of a compact potentiostat for an aptamer-based biosensor, suitable for point-of-care testing (POCT) applications. A potentiostat applies a pre-programmed time varying voltage to a set of electrodes that hold a biomolecular sample, and simultaneously monitors the resulting electrochemical signals. The potentiostat is designed to operate and communicate through a standard USB port of any computer. The sensor platform is composed of a 3-electrode system and constructed using microfabrication techniques; in conjunction with the potentiostat the device performs cyclic voltammetric tests on surface-bound, redox-labelled biomolecular samples. The performance of the system is compared to that of a commercial benchtop potentiostat.

Results of this research will contribute to the design of a stand-alone, USB powered, biomolecule detection system. Such a system may in turn form the basis of future hand-held, ultra-compact, point-of-care biosensors for disease screening and personal health care monitoring.

Keywords: Biosensor; Potentiostat; Cyclic voltammetry; 3-electrode electrochemical system; Redox reactions; Point-of-care diagnostics systems

DEDICATION

I would like to dedicate this thesis to my loving family, without whom I would not be who I am today.

ACKNOWLEDGEMENTS

I would like to thank my senior supervisor Dr. Ash M. Parameswaran for all his guidance and encouragement throughout my research. Most importantly, I would like to thank him for giving me the freedom to pursue my research with full support. I would also like to thank my supervisor Dr. Hogan Yu for all his guidance and feedback. Thank you to Dr. Marinko Sarunic for graciously agreeing to be my examiner for my thesis defence. And many thanks to Mike Sjoerdsma for his feedback and input on my thesis, and his encouragement throughout my research. I would also like to thank Cassie Ho and Yiting Tang for their patience and understanding while teaching me everything they could about electrochemistry. I thank both the microelectronics lab and the chemistry lab for all of their support, ideas and help throughout my research. And most importantly, thanks to my family for all their love and support.

TABLE OF CONTENTS

LIST OF FIGURES

LIST OF TABLES

LIST OF ACRONYMS

ADC Analog to digital converter

CE Counter electrode

CV Cyclic Voltammetry

CVs Cyclic Voltammograms

DAC Digital to analog converter

DNA Deoxyribonucleic acid

GUI Graphical user interface

PCB Printed circuit board

PCR Polymerase chain reaction

PDMS Polydimethylsiloxane

PMMA Poly(methy methacrylate)

POCT Point-of-care testing

RE Reference electrode

WE Working electrode

1: INTRODUCTION

Portable biosensors have become essential to the world of medicine, a need that materialized due to an ever increasing population and as a means to provide health care to all. Leland Clark of the Children's Hospital Research Foundation in Cincinnati developed the first biosensor in 1962, but it wasn't until 1975 that his discovery was commercialized [1]. Today, that first biosensor, better known as the glucose monitor, has provided millions of diabetics with independence, allowing them to monitor their disease at home, thereby decreasing their need for medical attention. The glucose monitor has also provided an immense aid to the government and health care system considering that "more than 20 people are diagnosed with diabetes every hour of every day" [2]. As such, the development of new biosensors for disease detection is of great interest.

Today, scientists and engineers are exploring the development of biosensors to perform protein detection as genomic research continues to discover thousands of proteins with potential diagnostic applications [3]. However, although the presence of these new protein biomarkers can be detected through specific optical binding assays (e.g., ELISA), producing portable biosensors of equal calibre and accuracy as the glucose monitor or the at-home pregnancy test, has yet to be realized. By creating a biosensor capable of detecting such biorecognition reactions, using off-the-shelf components and

powered only by USB connection, our work provides an economical solution to the issue of on-site protein biomarker detection.

1.1 Objectives

The objective of this work was to design a portable biosensor prototype that could perform electrochemical measurements for the purpose of medical diagnostics. The primary objective was to design a USB powered electronic circuit (known as a potentiostat) to execute a potential scan that would output resulting electrical current in real time. Numerous commercial instruments that perform such analysis are available; however, their size and cost inhibit their application for on-site testing [4]. In an attempt to overcome this obstacle, many portable designs have been presented [4-6], but they are still hindered by power supply requirements or methods of operation including data handling and display. Several designs require an external power supply and are, therefore, restricted to environments that can provide such a supply. Battery operated designs also exist, but they are inadequate in their data display: to conserve power they either display one data point at a time or none at all [5, 6]. An RS-232 connection is then required to upload the data to a Personal Computer (PC), where the results are analyzed at a later time [6, 7]. In either case, tests cannot be performed on-site concurrently with the data displayed in real time.

The secondary objective of this work was to design the measurement platform, or electrochemical cell, in which tests are performed. This system comprises three electrodes, namely a working, reference, and counter electrode, with electrical connections to the potentiostat circuit. The standard

electrochemical cell used for testing purposes in our lab only permits one working electrode to be tested at a time, and, since the insertion and removal of the working electrode causes the electrode to break roughly one out of four times, the cell is not appropriate for field work. Other portable designs of such systems do exist: the most commonly used portable electrochemical cell is a screen-printed disposable strip, a variation of which is used in conjunction with the glucose monitor. However, these strips are not commercially available and are costly unless mass produced**.** They also do not meet the surface area and material restrictions required for the working electrode for our application. To this end, miniaturized electrode sets were developed to provide an economical test platform for our prototype.

1.2 Scope

The scope of this work was to design a biosensor prototype and prove its functionality by performing electrochemical detection of lysozyme using a DNA aptamer – each of which were novel technologies. System calibration and analysis of repeatability of detection will be addressed in future work, which is beyond the scope of this thesis.

1.3 Thesis Outline

The research presented in this thesis focuses on the design and fabrication of both the portable potentiostat system as well as the miniaturized electrochemical cell. Chapter 2 provides an overview of electrochemistry and its applications to biosensor design. The design and implementation of the

biosensor prototype, as well as verification of the device's functionality, is discussed in chapter 3; chapter 4 covers all calibration and testing of the prototype that was completed. The final chapter presents conclusions and future work.

2: INTRODUCTION TO ELECTROCHEMISTRY AND ITS APPLICATIONS

2.1 Electrochemistry

Electrochemistry studies the electrical signals produced from a chemical reaction for analytical purposes. Of particular interests for electrochemistry are redox reactions, whereby one molecule undergoes oxidation (releasing electrons) and the other undergoes reduction (accepting electrons). When both reactions are present within a single system, a spontaneous current can be generated. This current produced between the two electrodes (conductive elements that hold the reactions and permit electron flow) placed in an electrolytic solution, can be measured. The electrodes must be connected only via an external circuit through which the electrons may travel. This setup is known as a *galvanic* or *voltaic* cell and is shown in Figure 1 [8]. The cadmium and silver-silver chloride electrode are placed into a solution of $CdCl_{2(aq)}$. As the cadmium undergoes oxidation, electrons are released and travel to the silver electrode through the external wire. Once they reach the AgCl coating, Ag^+ is reduced to Ag, which releases Cl^- ions into the solution. However, the reduction of Ag^+ is not forced to occur at the Ag electrode's surface, aqueous Ag^+ can react directly with the surface of the Cd electrode [8].

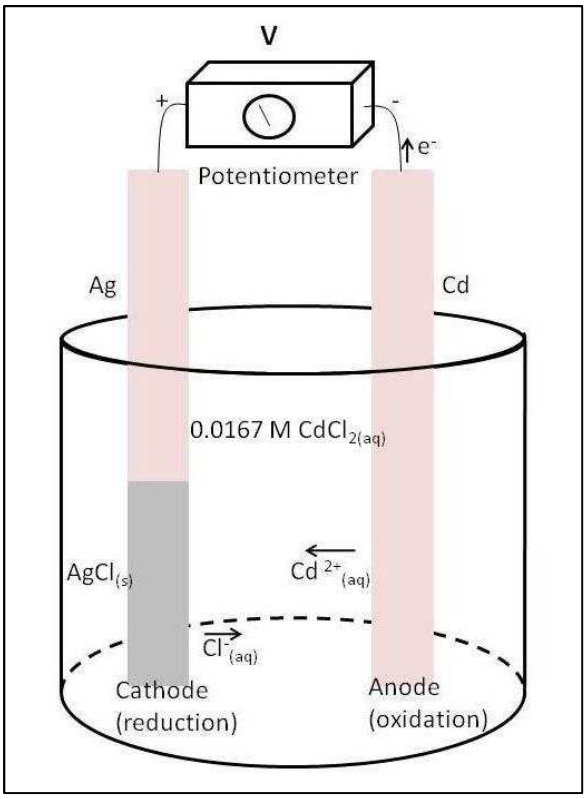

Figure 1: Galvanic cell - as the cadmium is oxidized, electrons travel through the potentiometer and reduce the silver chloride ions to solid silver at the electrode surface. Adapted from [8].

When the reaction is separated into two half-cells, the ions in solution can no longer react at the surface of the electrodes, therefore, the electrons are forced to travel through the external path which creates a manageable current. This setup is shown in Figure 2 [8].

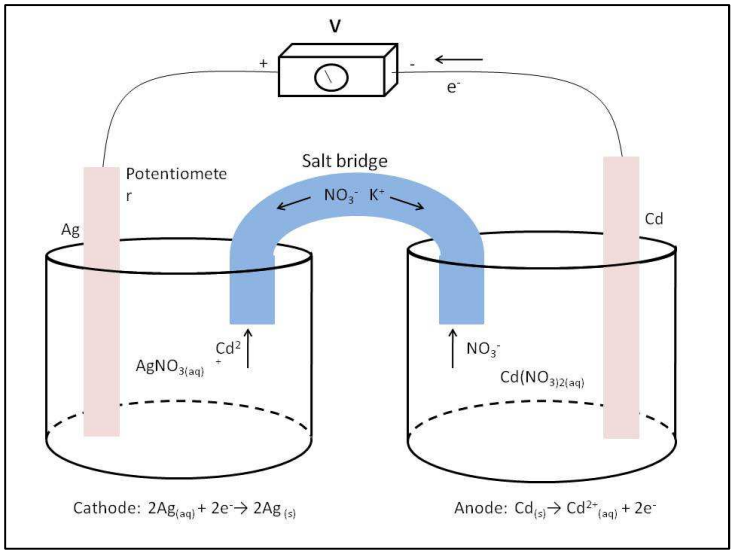

Figure 2: Two half cells - separating the reaction into two half cells will force the electrons to take the external path creating a stronger current.

As the electrons move from one electrode to the other via the external circuit, a potential difference will build. For the half-reaction

$$aA + ne^- \rightleftharpoons bB, \tag{1}$$

at 25 °C, the half-cell potential is given by the Nernst equation:

$$E = E^\circ - \frac{0.05916}{n} \log \frac{\mathcal{A}_\mathrm{B}^b}{\mathcal{A}_\mathrm{A}^a} \tag{2}$$

where E° is the standard reduction potential, n is the number of electrons in the half-reaction, and $\mathcal{A}_i$ is the activity of species i (or the effective concentration). Therefore, the half-reaction

$$2Ag^{+} + 2e^{-} \rightleftharpoons 2Ag_{(s)},$$

would result in a half-cell potential of

$$E = E^{\circ} - \frac{0.05916}{2} \log \frac{1}{[Ag^{+}]^2}.$$

Hence, the potential is concentration dependent. The resulting cell voltage (potential deference between the two half cells) can be used to determine chemical composition in the reaction; this practice is called potentiometry.

Potentiometry can be used to obtain quantitative information of an analyte. The analyte is an electroactive species meaning it can donate or accept electrons while interacting with an electrode's surface. By using analyte specific electrodes (or electrodes that respond specifically to a particular substance being analyzed), potentiometry can be used as a method of detection. As mentioned above, a galvanic cell consists of two electrodes. When performing potentiometry measurements on an analyte, the electrode that responds to the substance in question is the indicator or working electrode (WE). Common metals for working electrodes are platinum, gold, and various forms of carbon, such as glassy carbon and graphite. They are inert, and, therefore do not participate in the reaction; their sole purpose is to transmit electrons to and from entities in the

solution. The second electrode is the reference electrode (RE). It holds a stable potential during the redox reaction so that the resulting potential may be measured with respect to a known potential. One of the most commonly used reference electrodes, due to convenience, is a silver wire coated with silver chloride that resides in a saturated solution of potassium chloride. This solution ensures the chlorine ions are never depleted and the potential of the half-cell remains constant.

In order for a reaction to occur spontaneously, certain conditions must be met (see Appendix A). When a chemical reaction does not occur spontaneously, a voltage equal to

$$E = E(cathode) - E(anode) \quad (3)$$

must be applied to the system to force the reaction. This process is called electrolysis.

During electrolysis, the applied potential must be controlled. If the applied potential varies and reaches sufficient voltage to force another reaction from any other electroactive species present within the system, the resulting current will be affected. Consequently, incorrect conclusions may result. Therefore, the applied voltage must be measured accurately against a reference electrode. To ensure that the potential at the RE remains constant, the current at the RE must not fluctuate. To accomplish this steady current, a third electrode is introduced: the auxiliary or counter electrode (CE), which acts as a conductor and supplies or draws current from the system. Therefore, a voltage is applied between the WE

and RE, while a current runs between the WE and CE. The device that applies this voltage and reads the resulting current is called a potentiostat.

2.2 Methods of Analysis

The current produced from electrolysis is proportional to the concentration of the analyte. That is,

$$I \propto [C]_o - [C]_s, \tag{4}$$

where I is the limiting current, $[C]_o$ is the concentration of the bulk solution, and $[C]_s$ is the concentration of the solution at the surface of the electrode. Depending on the reaction setup and initial concentrations, $[C]_s \ll [C]_o$ or $[C]_s \gg [C]_o$. Therefore, the current can be governed by the analytes rate of diffusion, or the surface confined reaction, that is, how many available electrons are at the surface of the electrode, and how quickly they can be exchanged. These concepts form the basis for quantitative analysis by amperometry and voltammetry.

Amperometry applies a step voltage across the working and reference electrodes, and it measures the resulting current against time. The concentration of the electroactive species can then be calculated using

$$i = \frac{nFA\sqrt{D}C_{O_x}}{\sqrt{(\pi t)}}, \tag{5}$$

where n is the number of electrons transferred per electroactive molecule or ion; *F* is the Faraday constant; *A* is the area of the electrode surface in cm^2 ; *D* is the diffusion coefficient in cm^2/s; C_{Ox} is the concentration of the oxidized species in

mol/cm^3; and *t* is the time in seconds [9]. Unfortunately, amperometry cannot determine the kinetics of the electron transfer and hence the kinetics of the reaction. That is, it cannot determine whether a surface confined or diffusion controlled reaction has occurred; information obtained from amperometry is limited compared to that of voltammetry.

Instead of time, voltammetry studies the current against a change in voltage. Cyclic voltammetry linearly sweeps the applied voltage across the working and reference electrodes and back again creating a cycle, while measuring the current throughout the process. The results are plotted in a cyclic voltammogram; Figure 3 below shows the response of a reversible redox reaction for

$$O + ne^- \rightleftharpoons R. \tag{6}$$

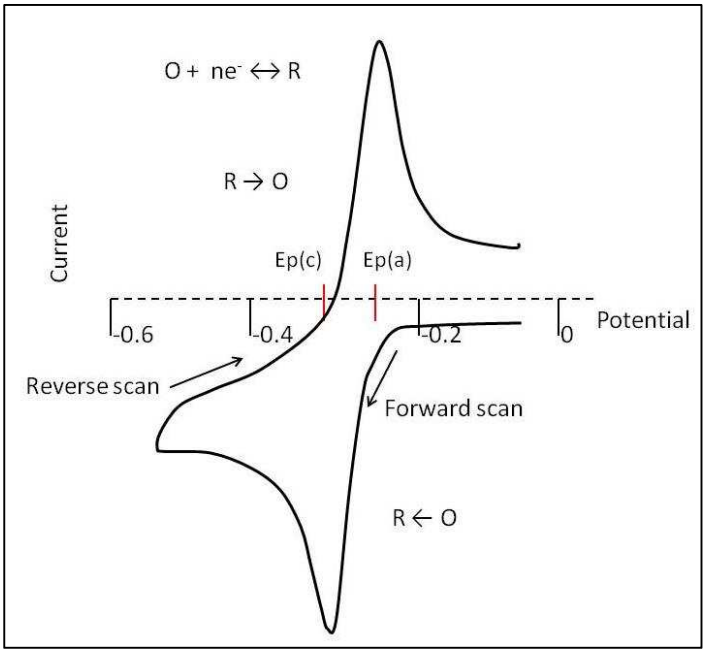

Figure 3: Cyclic voltammogram of a reversible reaction

As the voltage is decreased and swept towards the reduction potential of the system, electron transfer between the electrode and the oxidized species begins. This current continues to increase until a cathodic peak is observed, corresponding to a peak potential of $E_{p(c)}$ [9]. Past this potential, the oxidized species becomes depleted and the current decreases [9]. The voltage is then reversed and swept towards the oxidation potential. This change in potential forces the reverse reaction whereby the reduced species becomes oxidized, resulting in an anodic peak at $E_{p(a)}$. Both the peak currents and peak potentials can be drawn from a cyclic voltammogram; the charge is calculated by integrating the area under the curve. Using the charge calculated we can determine the surface density of the species on the electrode using

$$\Gamma = \frac{Q}{nFA}, \tag{7}$$

where Q is the peak area, n is the number of valence electrons, F is the Faraday constant and A is the area of the working electrode. Kinetics of the reaction can also be determined by reviewing several reactions at different rates and comparing peak potentials and currents. Because cyclic voltammetry can extract more information from the reaction, we chose to implement this method of analysis.

2.3 Biosensors and Electrochemistry

A biomarker is a substance, often a protein, which is indicative of the onset or predisposition of disease [10]; a biosensor is a device that is used for the detection of such biomarkers. Because electrochemical detection methods, such

as cyclic voltammetry, can be used to confirm the presence of analytes or biomarkers within a solution, these methods hold great potential in the creation of new biosensors. Biosensors are a two part system: a) the cell or platform that enables detection of the analyte (such as a biomarker) through a chemical reaction, and b) the transducer which converts the results of such a reaction into a quantitative signal [11]. To detect the analyte, biosensors often draw on natural biological reactions; therefore, a potential exists to develop different devices to detect all possible biomarkers. Natural biological reactions, such as the antibody/antigen reaction, are governed by selective molecular binding. That is, they operate on a “lock and key” interaction. For example, an antibody possesses a ‘lock’, a particularly shaped binding site that will only bind to a specific antigen, see Figure 4.

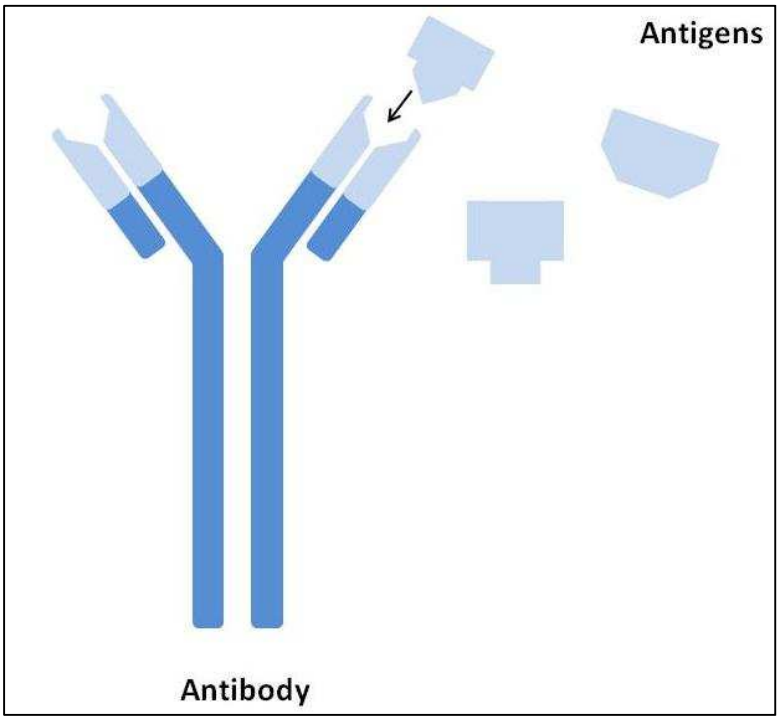

Figure 4: Antibody and antigens – the correct combination forms a lock and key situation whereby only the correct antigen will cause the antibody to bind and react to its presence.

Once the specific antigen has “locked” itself into the antibody, only then will the antigen be identified. Most biosensors mimic such reactions by monitoring selective binding between a targeted protein and a bio-recognition reagent. The bio-recognition reagent is usually bound to the electrode or immobilized in a membrane [12]. The analyte, most often contained in bodily fluids, is then introduced into the environment, and reacts with the bio-recognition element. This reaction can be direct binding of the bio-recognition element and the analyte, or a catalytic interaction whereby new products are produced. In either case, the reaction is driven by an applied voltage, and the resulting current is analyzed.

Once the biorecognition reaction has been established, the transducer must be developed. At present, laboratory assays are still the most common routine process of determining the presence and abundance of a protein biomarker. This process involves introducing the sample into an environment that will facilitate a reaction between the sample and a known substance. These techniques require the use of highly trained laboratory technicians to perform sample handling including collection and preparation as well as processing and analysis once the reaction has occurred. The whole procedure requires a minimum of one day. Adapting these protocols to a portable sensor “has always been the ideal situation, but the complexity of most diagnostic tests and the difficulty of interpreting the results correctly have kept them [in] laboratories and hospitals” [13]. Therefore, simpler methods of detection are being implemented. While both optical and electrochemical approaches are two very plausible techniques, electrochemical sensors have a greater capacity for miniaturization due to their ability for measuring direct electrical signal output.

The most successful electrochemical biosensors to date are the glucose monitor and the Clark electrode. In both tests, a redox reaction takes place between the analyte and the biorecognition element. In both cases, amperometry is used to apply a known potential to the system; the resulting current is measured and used to determine the concentration of the analyte. With the above two sensors, the concentration of glucose and oxygen within the blood can be determined, respectively. Although the test is quite simple, manufacturing monitors that require little or no calibration is not [8].

2.4 Current Biosensor Developments

Many genetic disorders as well as the onset of cancer and other diseases can be detected by DNA mutations and abnormal levels of certain proteins within the blood. Although immense progress has been made towards developing electrochemical DNA biosensors, alongside portability, the issue of obtaining adequate sensitivity and selectivity must also be addressed before these sensors can become commercialized [11]. In the case of gene detection, many target DNA strands are in low concentration and must be amplified using a process called polymerase chain reaction (PCR). While this process does increase the number of target DNA molecules within a sample, it will also amplify the number of contaminants [11], and requires one day to complete. If the sensitivity were increased, amplification could be lessened or avoided altogether. Because biosensors produce results based on assumed reactions, the binding criteria of said reactions must be highly specific to avoid false diagnoses

2.5 Lysozyme Detection

Our biosensor design was verified by testing for lysozyme detection. “Lysozyme is a ubiquitous protein in mammals and is often termed [the] “body’s own antibiotic” [15]. It is an enzyme that helps the body to fight off infection by breaking down the cell walls of bacteria. We performed lysozyme detection by using lysozyme aptamer as described by Cheng et al. in [15]. . Aptamers are nucleic acids and are therefore composed of a linear sequence of the same nucleotides that make up DNA and RNA. They are selected in vitro from large pools of random sequences; due to their three dimensional shape, they perform

highly sensitive shape-specific recognition of their target molecules [14, 15]. In addition, since they are selected from pools of 10^{12}-10^{15} sequences, in theory, aptamers can be found to bind to virtually any possible biomarker; therefore, they possess great potential in the development of biosensors [16, 17].

By showing that our design can detect lysozyme at a concentration of 0.5 ug/mL, we will show that is has the required sensitivity and functionality to perform any similar protein detection tests.

3: PROTOTYPE DEVELOPMENT

Benchtop potentiostat systems can perform numerous electrochemical analysis techniques within a wide range of parameters including variations of signal output and data interpretation. However, our initial potentiostat system design is only required to perform cyclic voltammetry. As such, many costs were omitted by minimizing system requirements and controls; these design parameters also allowed for minimization of the device size.

To perform cyclic voltammetry, a voltage is applied to the working electrode, momentarily held at an initial voltage, and linearly decreased until a vertex voltage is reached. The voltage is then reversed and swept back towards the initial value. Throughout this cycle, electron transfer occurs within the electrochemical cell; this current is measured at the working electrode and recorded for analysis. This chapter discusses how the potentiostat was designed to accomplish these tasks.

3.1 Circuit Design and Fabrication

The potentiostat circuit endured several redesigns before a final design was established. However, in every design, a microcontroller and a digital counter governed the circuit.

The voltage sweep applied to the working electrode is generated by the microcontroller (in this design, an Atmega644, Atmel Corporation) which instructs

the counter to count from 255 to 0 corresponding to a voltage of +5 V to 0 V, respectively. The first version of the potentiostat design was completed on a breadboard. Photographs of the circuit and setup are shown in Figure 5 and Figure 6, and a circuit diagram is shown in Figure 7.

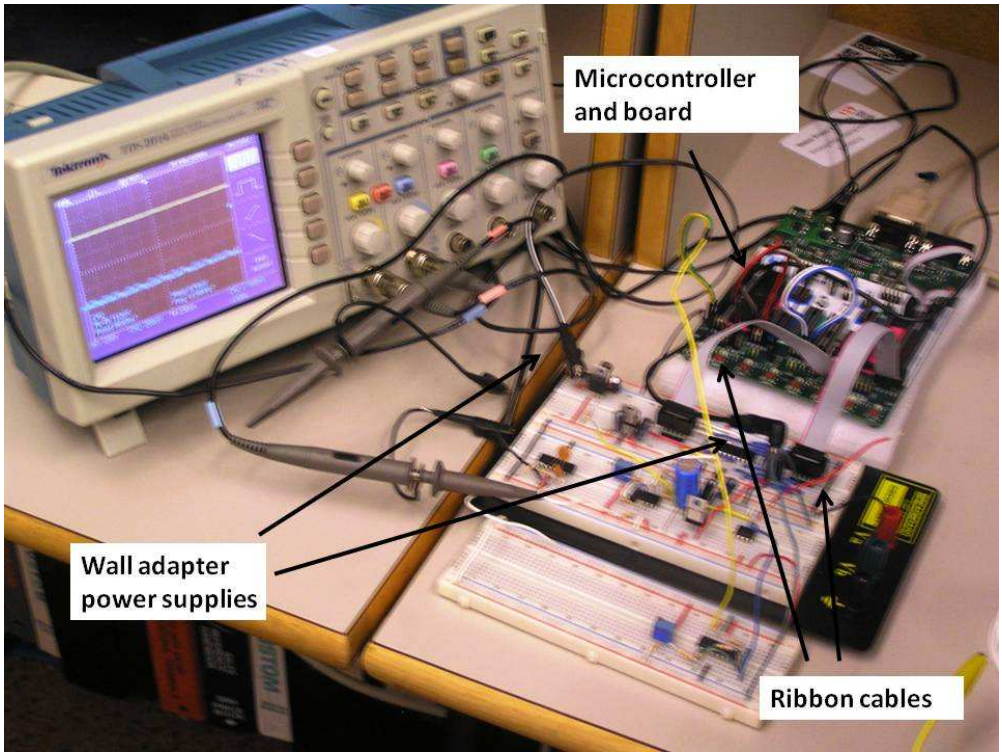

Figure 5: The entire setup for the first potentiostat design – the microcontroller board is connected via two ribbon cables to the main breadboard. Three external power supplies are also connected (two shown here).

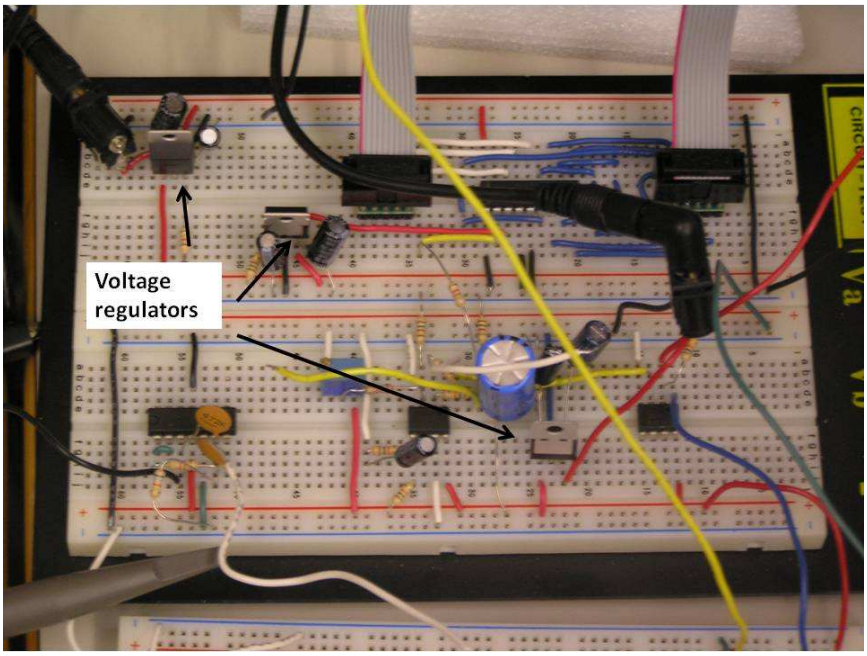

Figure 6: Close up of the main circuit board shown in Figure 5. Three voltage regulators are connected to the three external power supplies.

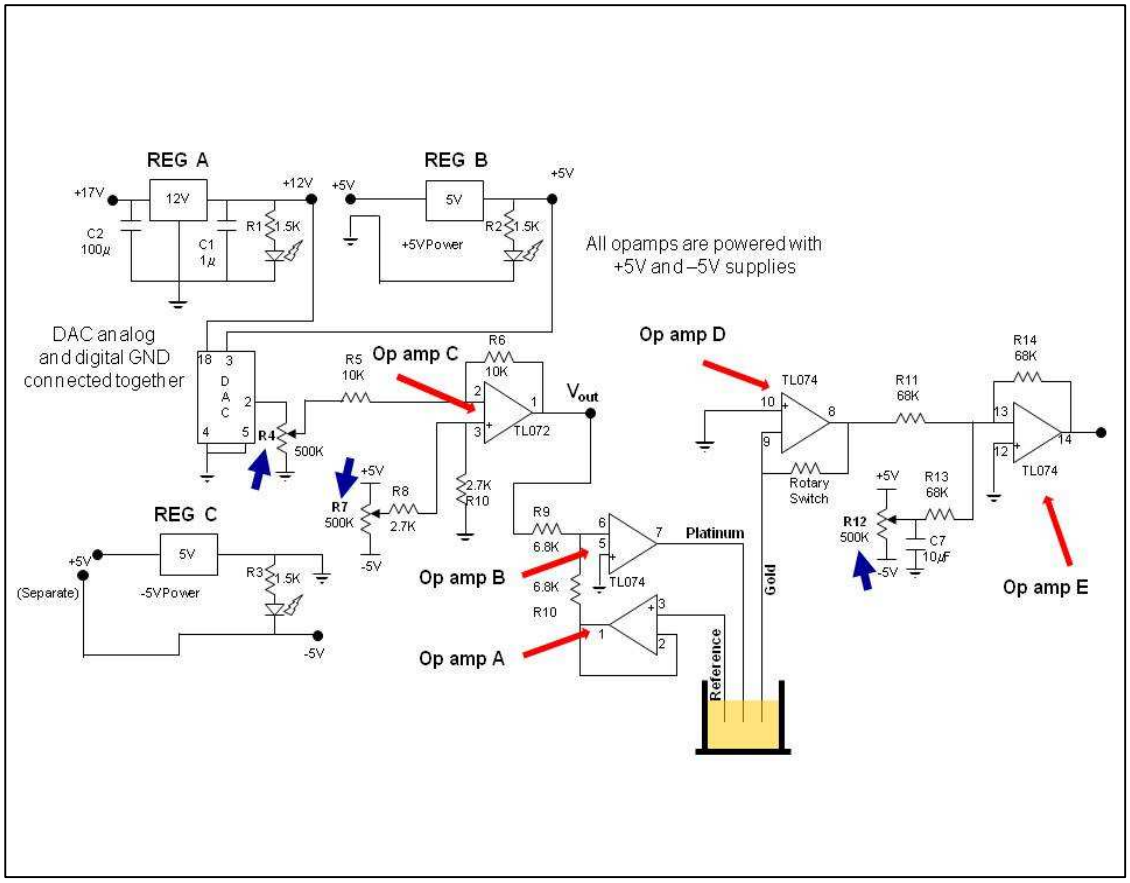

Figure 7: Schematic diagram of the first potentiostat design shown in Figure 6.

The 17 V wall adapter power supply generates a regulated +12 V output from the voltage regulator denoted as Reg A in Figure 7. This voltage powers the digital to analog controller or DAC. All other components are powered with regulated +5 V or -5 V from Reg B and Reg C, respectively, which are powered by two 9 V wall adapters. The voltage sweep generated by the microcontroller is fed to the DAC, which converts the digital signal into an analog output, namely a triangular wave. This signal has a magnitude of 5 V, and sweeps between 0 V and +5 V. However, the user can select the desired voltage sweep (with a maximum magnitude of 5 V) by adjusting two variable resistors. The resistor denoted R_4 is

used to attenuate the signal to the desired magnitude. The resistor denoted R_7, along with op amp C, creates a level shifter: the op amp is configured as a difference amplifier, and, in this setup, the output is governed by

$$V_{out} = V_2 - V_1. \tag{8}$$

By allowing the user to change the voltage at the non-inverting input, the attenuated signal can be shifted into the appropriate range. The resulting voltage, V_{out}, is applied to the reference electrode at op amp A and to the current buffer [18], op amp B. The reference electrode is connected to the non-inverting input of op amp A, which has near infinite input resistance, therefore no significant current transfer (less than 10 nA) can occur at this electrode. The counter electrode is connected to the output of op amp B, which is isolated from the inputs of op amp B. As such, the counter electrode can supply any required current (constrained only by the source voltage) to the electrochemical system.

The current generated from the electrochemical cell is forced to travel to the working electrode connected to the current to voltage converter (or I-to-V converter) denoted by op amp D. The rotary switch at op amp D allows the user to select an appropriate amplification depending on the current range. The output voltage is then converted back into a digital signal via the analog to digital converter (ADC). However, because the ADC can only accept voltages within a range of 0 V to +5 V, the output voltage must be manipulated to ensure functionality. Therefore, another variable resistor, R_{12}, is used to shift the voltage into the 0 V to +5 V range using the configuration of a summing amplifier at op

amp E. In this preliminary design, the digital signal was then uploaded to a PC via a USB to a serial communication interface; in this case, Hyper Terminal.

Although this circuit performed the correct functions, this design had many issues; the most prevalent being noise. An oscilloscope was used to capture a cyclic voltammogram for potassium ferricyanide obtained with this circuit, which is shown in Figure 8.

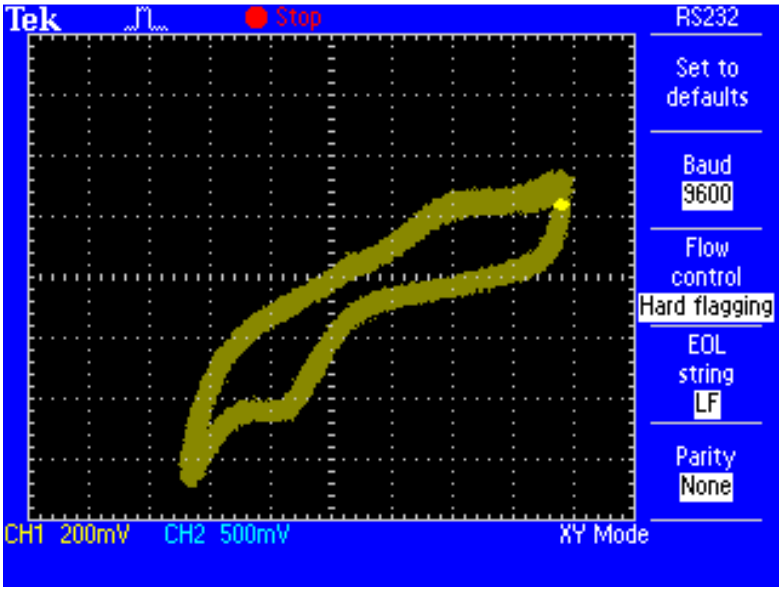

Figure 8: Cyclic voltammogram of potassium ferricyanide.

We assumed much of the noise was due to the breadboard and the excess wiring that was required for component connections. To address this issue and confirm the source of the noise, the breadboard was eliminated in the second design by transferring the circuit to a printed circuit board or PCB. An Arduino Duemilanove (Arduino™) microcontroller board containing an ATmega168 microcontroller was used in this implementation in an attempt to minimize the device size. This second design is shown in Figure 9.

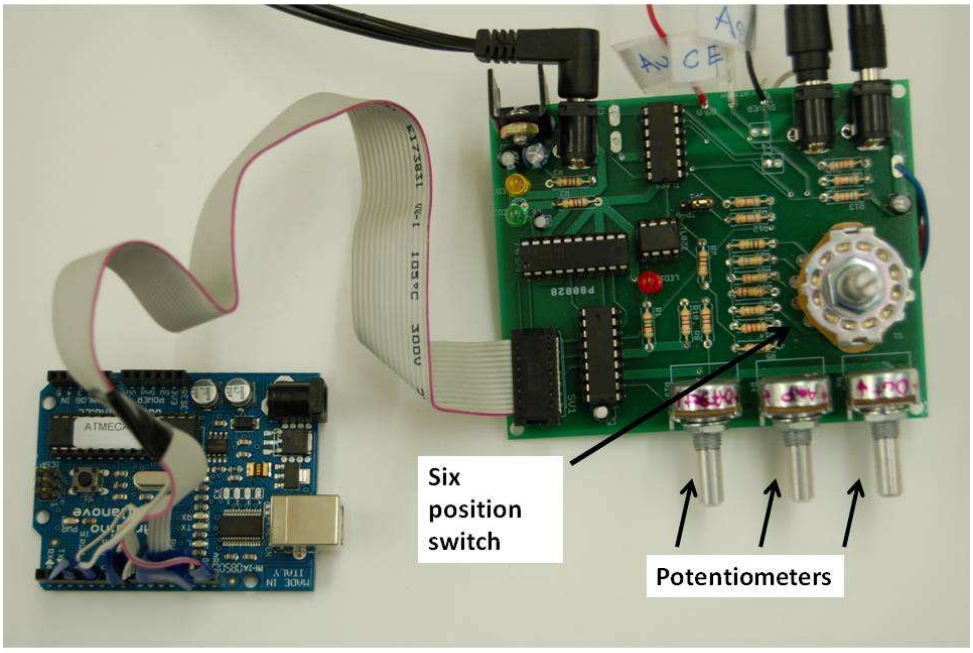

Figure 9: Second circuit design, circuit mounted on to a PCB.

In Figure 9, the three potentiometers serve the same purpose as the three variable resistors in the first design that were used to adjust the magnitude and the offset voltage of the input wave, as well as the level of the output signal. The potentiometers were used to provide more user friendly controls. In addition, the fourth variable resistor was replaced with a six position rotary switch to allow the user to select between six levels of magnification as the signal passes across the I-to-V converter. To test circuit functionality, cyclic voltammograms were obtained from a potassium ferricyanide solution using both the portable potentiostat as well as a CHI 1040 benchtop potentiostat (CH Instruments, Inc.). The results are compared below in Figure 10.

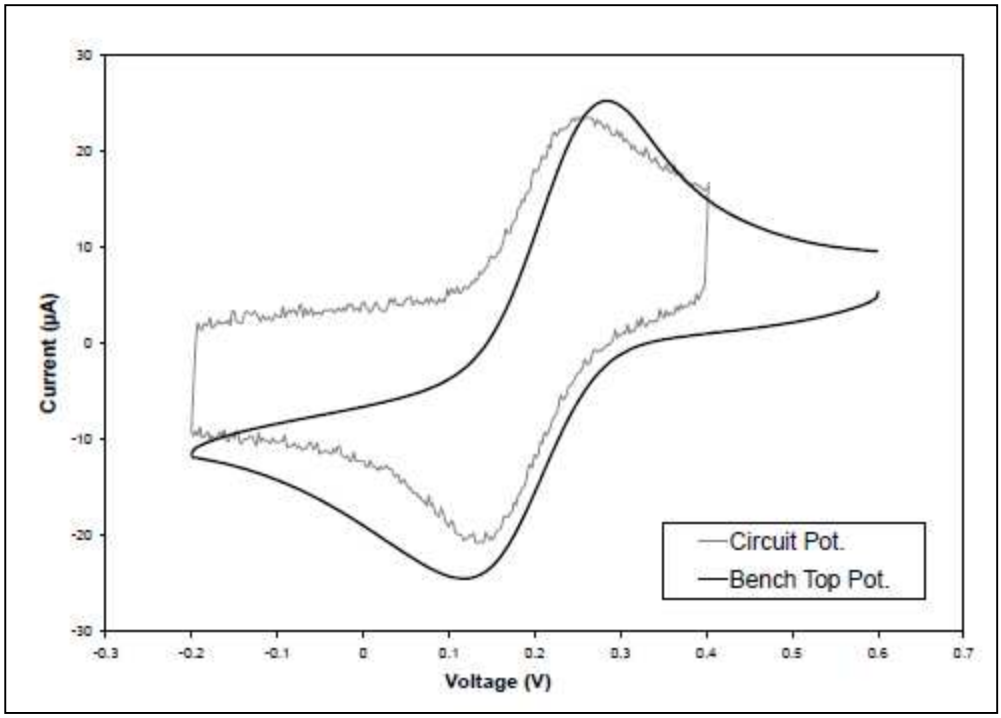

Figure 10: Benchtop vs portable potentiostat – Cyclic voltammograms of 1 mM potassium ferricyanide in 100 mM sodium chloride obtained from the first iteration of the portable potentiostat mounted on a PCB compared to the results of a benchtop system.

The signals display similar shape and undergo oxidation and reduction at potentials that differ by only 0.02 V, a shift that was most likely due to miscalculations when applying the DC offset to the digital data. The oxidation and reduction peak heights also differ by 3.8 μA. This difference is attributed to the calibration and data handling of the portable potentiostat. Although this second design was much more robust than the first, the results revealed that the breadboard was not the only cause of noise. Therefore, a hardware redesign was implemented to eliminate components possibly attributing to noise issues and to facilitate portability by reducing the overall size of the circuit.

The first issue addressed was portability. In order to allow for on-site testing, the external power supplies had to be eliminated. As a result, the entire circuit was redesigned to operate between 0 V and +5 V so that it could be powered by a USB connection. The second issue addressed was the number of stages or op amps within the circuit; every op amp amplifies the noise already present in the input signal and introduces additional noise to the output signal. Therefore, fewer stages result in a cleaner signal. The first op amp eliminated was op amp E used to shift the output voltage into the appropriate range for the ADC. As previously mentioned, the ADC can only accept voltages within a range of 0 V to +5 V. Therefore, to address the issue of negative currents at the WE and hence negative voltages at the input to the ADC, a virtual ground (GND_v) was introduced such that

$$GND_{V=}\frac{V_{CC}}{2}. \tag{9}$$

With this implementation, any voltage greater than $V_{CC}/2$ is seen as a positive voltage and any voltage below $V_{CC}/2$ is likewise negative. These changes are reflected in the circuit diagram shown below in Figure 11.

The virtual ground was created by using a voltage divider between V_{CC} and 0 V, and applying this voltage to the non-inverting input of op amp 5. The output, equal to GND_V, was then used as the ground voltage for the analog side of the circuit.

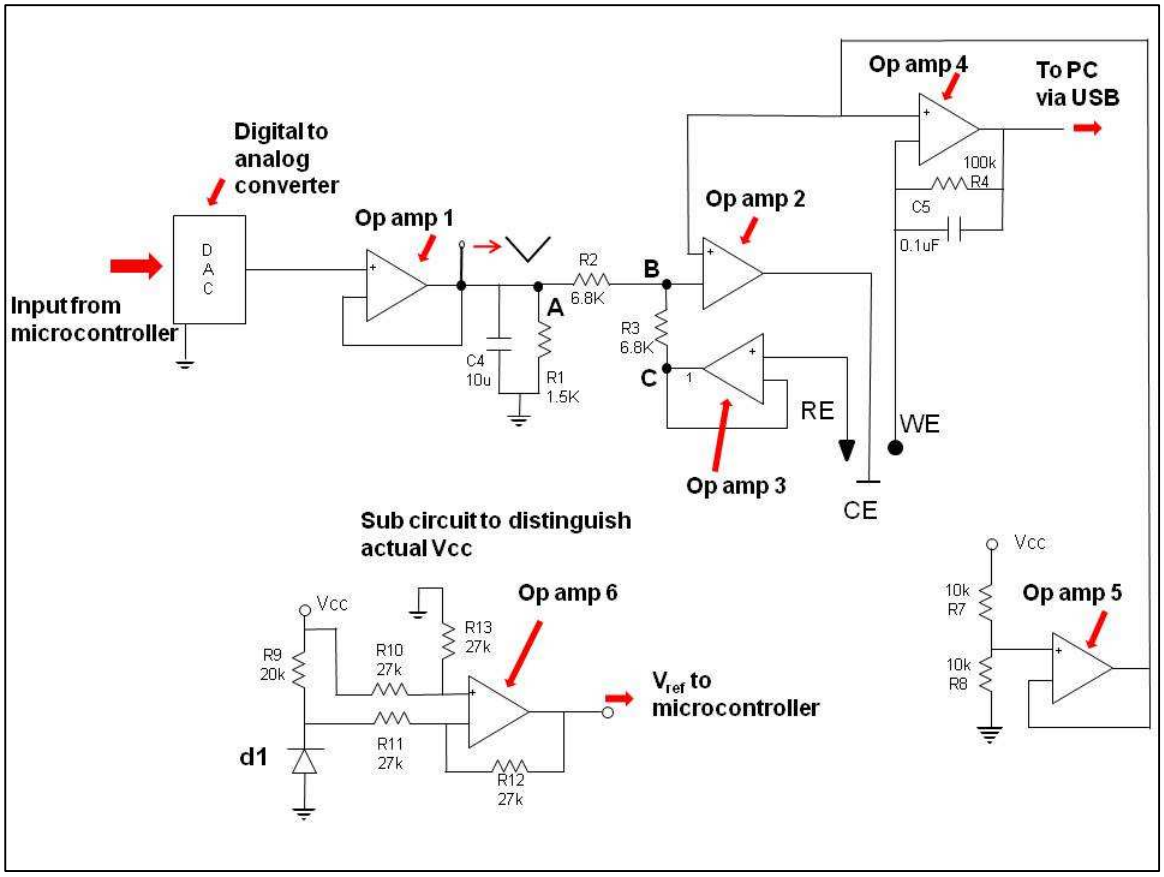

Figure 11: Portable potentiostat circuit diagram - new implementation powered by USB; virtual ground and subcircuit to determine actual V_{cc}.

With this implementation, the ADC can accept all output from the I-to-V converter directly. The digital portion of the circuit was mounted on a PCB, while the analog circuit was constructed on a breadboard. This arrangement allowed for further testing and analysis of the analog circuit to ensure proper functionality. The only issue that arose was the uncertainty of V_{CC}. Different USB ports produce slightly different outputs – an issue that affected the accuracy of the resulting current since all data is scaled proportionally to V_{CC}. To rectify this issue, an additional sub-circuit was introduced as shown above in Figure 11. A known voltage is produced across diode d1, which is subtracted from V_{CC} at the output of op amp

6. This voltage is read by the microcontroller and used to compute the actual V_{CC} from

$$\frac{(V_{CC}-V_Z)}{V_{CC}} = \frac{Read_{V_{CC}}}{1023} \Rightarrow V_{CC} = \frac{V_Z * 1023}{1023 - Read_{V_{CC}}} \quad (10)$$

Using this computed V_{CC}, both the input and output voltages were correctly scaled from their digital values to their corresponding voltage levels.

Next we removed the attenuation and level shifting op amps immediately following the digital counter output. Instead of generating a triangular signal with a magnitude of 5 V from the counter, the microcontroller was reprogrammed to initiate and terminate counting within the 0-255 steps, depending upon the user's input (via potentiometers) of initial and peak voltages. In addition to the op amps, we suspected the rotary switch was also contributing to the noise issue. For biosensor applications, we expect the output current to be within the range of microamps or less; therefore, the rotary switch and the six related resistors were removed and replaced with a 100 kΩ resistor. Once all the aforementioned op amps were removed, as well as the power supplies and variable resistors, the circuit became much more compact as shown below in Figure 12.

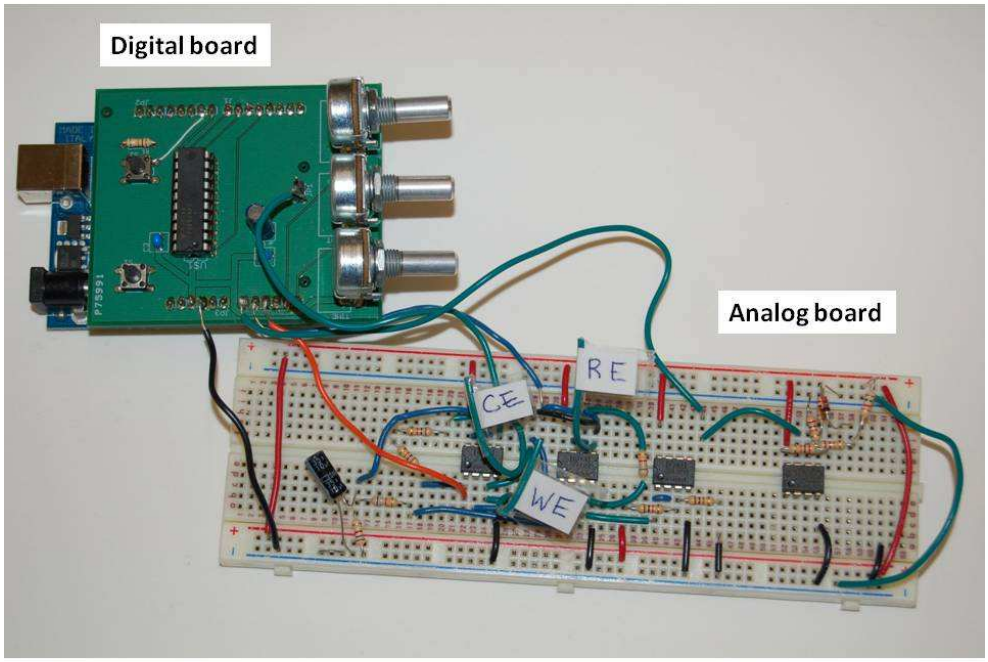

Figure 12: USB powered portable potentiostat: digital circuit mounted on PCB, analog circuit on breadboard to allow verification of the virtual ground and the 0-5 V operation.

Once the third design was verified, the bread-boarded analog circuit was implemented onto a PCB. In order to further minimize the circuit size and signal noise, we eliminated the ribbon cable connecting the microcontroller board to the circuit. Instead, pins were inserted into the top of the new PCB such that the microcontroller board could connect directly to the potentiostat circuit. A start and reset button were also implemented to provide more user control. The final design is shown in Figure 13, while results obtained from potassium ferricyanide CV tests are shown in Figure 14 and Figure 15.

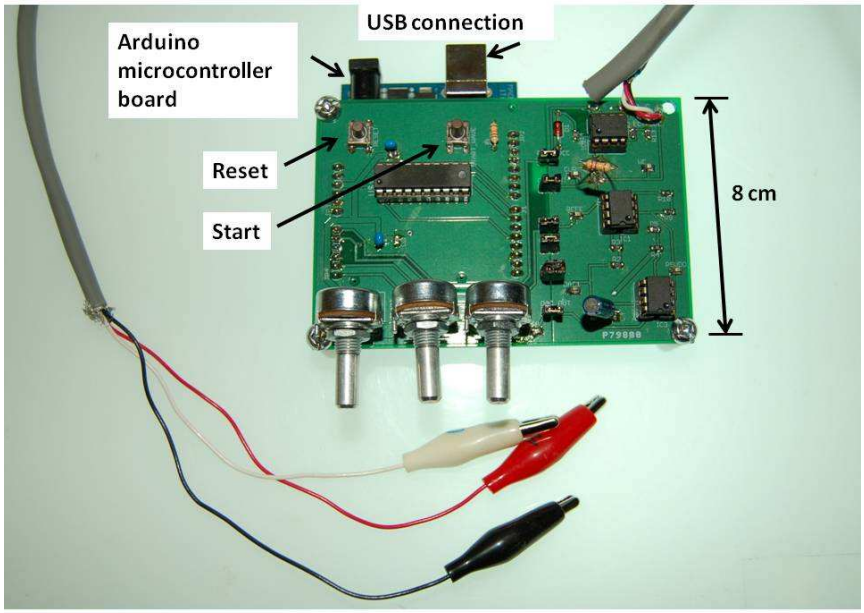

Figure 13: Final circuit design – Arduino Duemilanove microcontroller board attached underneath, digital and analog circuits implemented on one PCB powered by USB.

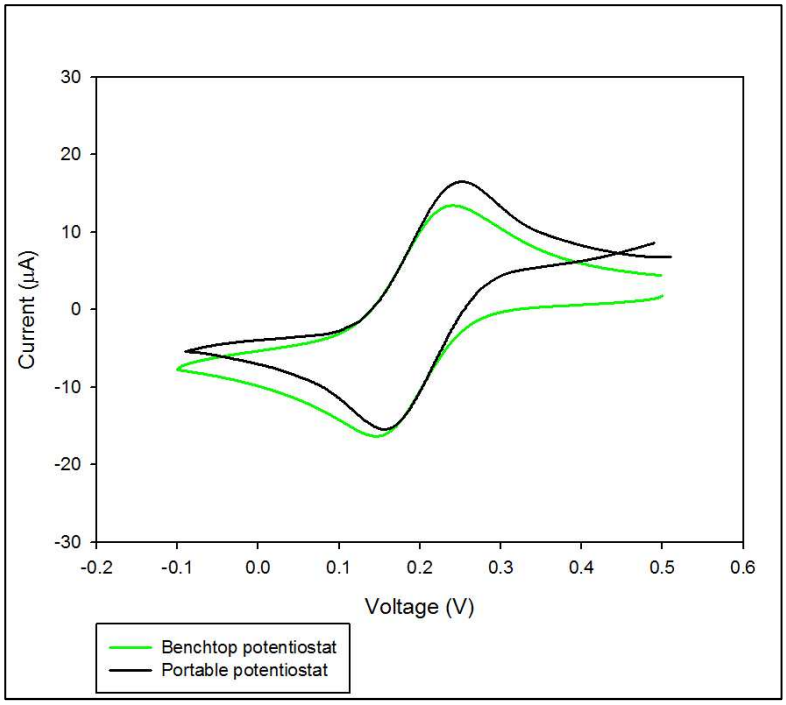

Figure 14: CV curves of 1 mM $K_3Fe(CN)_6$ in 100 mM NaCl on a gold electrode obtained with a benchtop and the portable potentiostat, respectively. The scan rate was 50 mV/s in both cases.

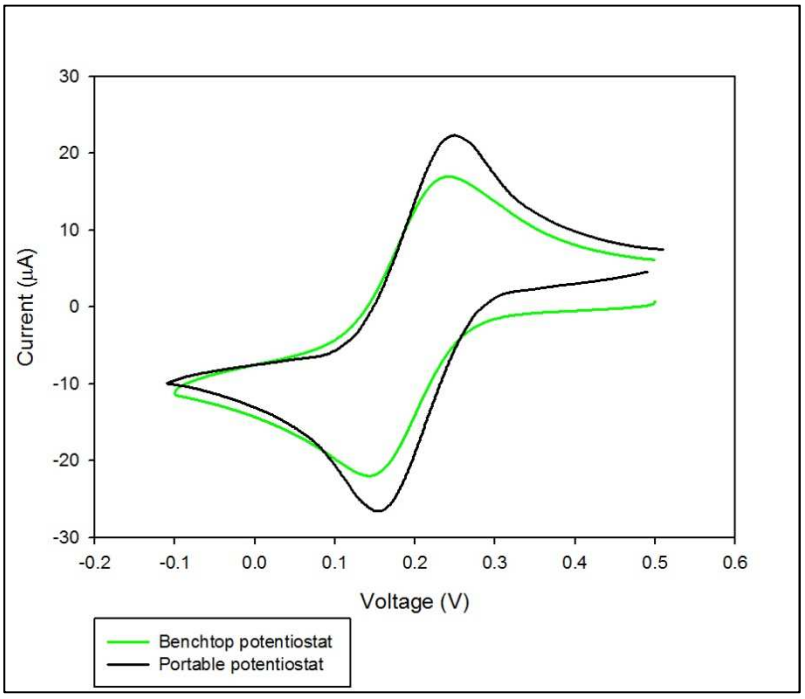

Figure 15: CV curves of 1 mM $K_3Fe(CN)_6$ in 100 mM NaCl on a gold electrode at a scan rate of 100 mV/s.

At a higher scan rate, the electron flow occurs more quickly. As a result, the peak current is 11.2 μA greater at 100 mV/s than at 50 mV/s. Comparing the cyclic voltammograms obtained from the two systems, a slight difference can be seen in their shape, however, they are comparable: the portable potentiostat is correctly applying the voltage sweep and recording the resulting reaction. The difference in peak height between the two systems is attributed to data interpretation and calibration. Because the internal circuitry of the benchtop system is unknown, comparing signal manipulation is not possible. However, if required, in future the software handling the data received from the portable potentiostat could be altered to calibrate the results and cause the output to mimic the benchtop system's results. In this work, the peak change as a function of the analyte concentration is of interest, and, therefore, the slight discrepancy between the two systems' results is not a concern. What is of concern is whether a change in the cathodic peak can be distinguished when using the portable potentiostat system to perform cyclic voltammetry on different solutions or solutions of different concentrations.

The current obtained from performing cyclic voltammetry tests on a lysozyme aptamer system is ten to thirty times lower in magnitude than the current obtained from a potassium ferricyanide reaction [15] . Because the peak current increases with scan rate, it is advantageous to be able to use higher scan rates so that the changes in current can be distinguished more easily as different concentrations of lysozyme are tested. Therefore, a software modification was

implemented and tested on a potassium ferricyanide solution. The results are shown in Figure 16 and Figure 17.

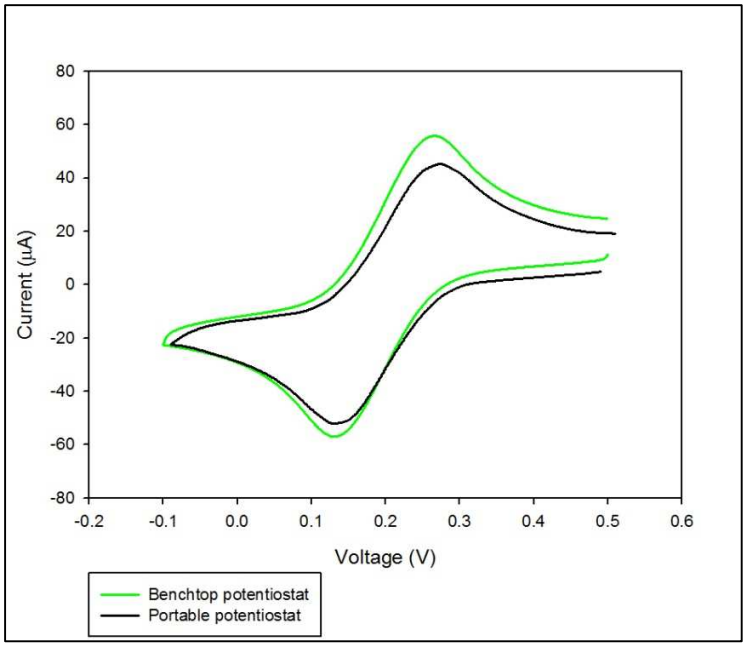

Figure 16: CV curves of 1 mM $K_3Fe(CN)_6$ in 100 mM NaCl on a gold electrode obtained with a benchtop and the portable potentiostat, respectively. The scan rate was 400 mV/s in both cases.

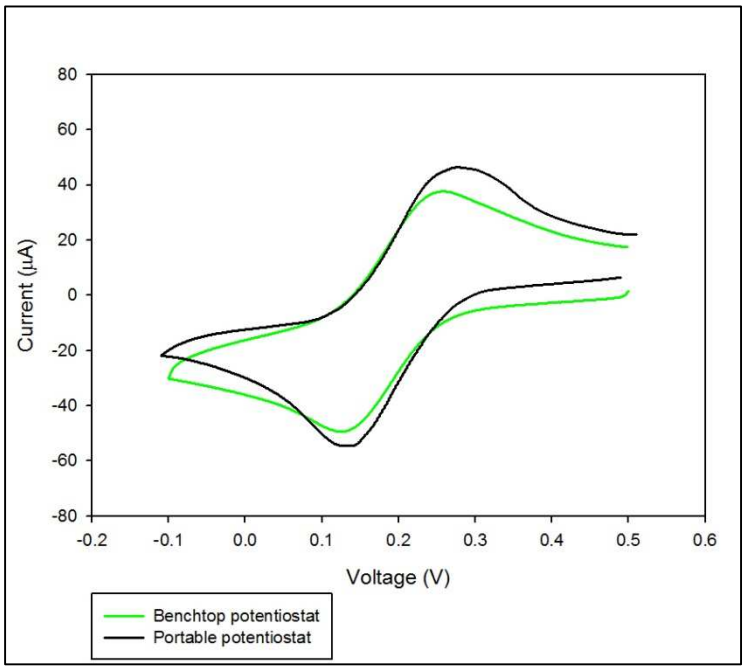

Figure 17: CV curves of 1 mM $K_3Fe(CN)_6$ in 100 mM NaCl at a scan rate of 500 mV/s.

Because the maximum operating voltage of the system is 5 V, the system will saturate when the I-to-V converter attempts to convert a current to a voltage greater than 5 V. At a scan rate of 500 mV/s, the current produced from the potassium ferricyanide reaction is too high and causes the I-to-V converter at op amp 4 to saturate. This saturation is shown in Figure 17, where the peaks of the CV have been cut off. However, we assumed that since the current produced during lysozyme detection is at least an order of magnitude lower than the current produced from the ferricyanide reaction, saturation would not be an issue.

3.2 Potentiostat Software

Two software programs were written to control the portable potentiostat: the software used to program the microcontroller and the digital circuit, and the software used to capture the output data and plot the results in real time. The following sections give a brief description of each program while Appendix B contains all code and comments in further detail.

3.2.1 Microcontroller

The microcontroller software was written in the Arduino 0019 compiler provided by Arduino™. The program consists of two parts: generating a voltage sweep to output to the analog circuit, and retrieving the output current received at the ADC. The first task is established with a counter and a while loop. Once the user has input an initial and peak voltage, and the start button has been pushed, the counter begins counting until the initial voltage (corresponding to a number

between 0 and 255) is reached. At this moment, the output of the counter is enabled. The counter continues to count down until the peak voltage is reached, and then begins to count upwards. Once the initial voltage is once again achieved, the loop terminates. The second task is accomplished by a series of analog reads and an averaging algorithm. The output of the ADC is read eight times per step of the voltage sweep; the weighted average is computed for both the applied voltage as well as the resulting current. The communication software, described in the following section, retrieves these values and creates a plot in real time.

3.2.2 GUI and Communication Software

The graphical user interface (GUI) was provided by Parallax Inc.: a Microsoft Excel add-in called Parallax Data Aquisition, or PLX-DAQ, which is used to upload data retrieved by a microcontroller to an Excel spreadsheet in real time. The add-in can be found free at parallax.com [19].

The GUI was implemented to allow the user to see what values are being selected by the potentiometers, as well as to initiate and terminate connection with the device. The voltage applied to the electrochemical cell, as well as the current generated at the working electrode, were updated to an Excel spreadsheet and plotted in real time. The user may also clear the data from the spreadsheet at any time.

3.3 Electrochemical Test Platform

Our biosensor prototype performs cyclic voltammetry and, therefore, required a portable three electrode test platform consisting of the working, reference, and counter electrodes, as well as an enclosure where the electrolytic solutions are held to maintain contact with the electrode system. This section describes the fabrication of the electrodes as well as the electrochemical cell.

3.3.1 Electrode Fabrication

The following sections describe the fabrication process of the working electrodes, as well as the reference and counter electrodes. The working electrodes were fabricated using photolithographic techniques; a brief description of the method used is given below; refer to Appendix D for greater detail.

3.3.1.1 Working Electrode Fabrication

In this preliminary stage, the gold working electrodes were fabricated on standard 3”x1” or 7.62 cm x 2.54 cm glass slides. Gold was chosen as the working electrode material because it is easy to clean and easy to pattern using photolithographic techniques, it is inert and therefore can be used for experimentation under atmospheric conditions, but most importantly, it forms a strong bond with a thiol group, the linker element that tethers the lysozyme aptamer. [20, 21]

Our first method of fabrication occurred as follows. A standard 3”x1” glass slide was cleaned using the RCA-1 procedure (see Appendix C) to remove organic contaminants such as dust or grease. Next, a 50 nm layer of chromium,

followed by a 50 nm layer of gold were sputtered on to the slide. Chromium was used because gold does not adhere well to glass. The slides were then spin coated with a layer of positive photoresist, and soft baked before patterned using a UV exposure and the mask shown in Figure 18. There are nine working electrodes on this mask. The contact pads were patterned along the edge of the slide so that an IC test clip could be placed into contact with all electrodes at the same time.

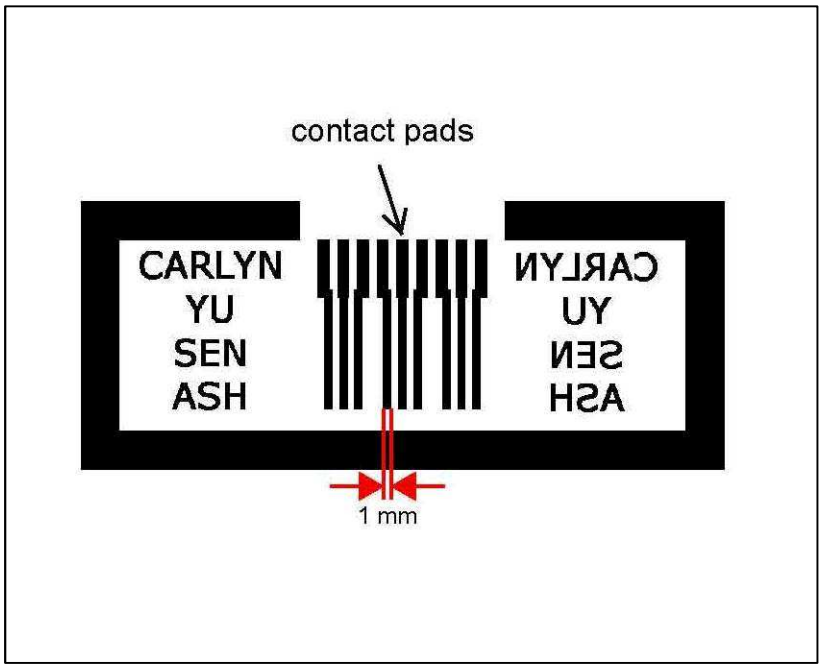

Figure 18: First mask used to pattern working electrodes on standard 3”x1" glass slide.

The slides were then developed to remove excess photoresist. To remove the unwanted metal, a gold and chrome etchant were used. Finally, a second UV exposure was used to remove the remaining photoresist from the gold electrodes.

We quickly realized this design had many flaws. First, the IC test clip that was used to make electrical connections to the electrodes would slide along the glass during testing. The proximity of the electrodes did not allow for alternate electrical connections to be made without causing a short between electrodes. Second, before the working electrodes are used for electrochemical testing, they must be cleaned in a freshly prepared solution of piranha (3:1 mixture of concentrated H_2SO_4 and 30% H_2O_2) at 90°C for 8 min. This solution is a strong oxidizer and, therefore, removes organic residues from the gold surface, but it is also highly acidic. The 50 nm layer of gold would not withstand the solution without causing slight surface abrasions that affected the ability of the thiolated DNA aptamer to bind to the gold. As a result, pre-coated, 10/90 nm chrome/gold glass slides from Evaporated Metal Films Inc. were used thereafter.

In order to ensure no cross contamination between electrodes, and to prevent any electrical connection shorts, the mask shown in Figure 19 was used to pattern the electrodes onto the pre-coated slides. See Appendix C for the detailed recipe. The working electrode slide patterned with this mask is shown in Figure 20.

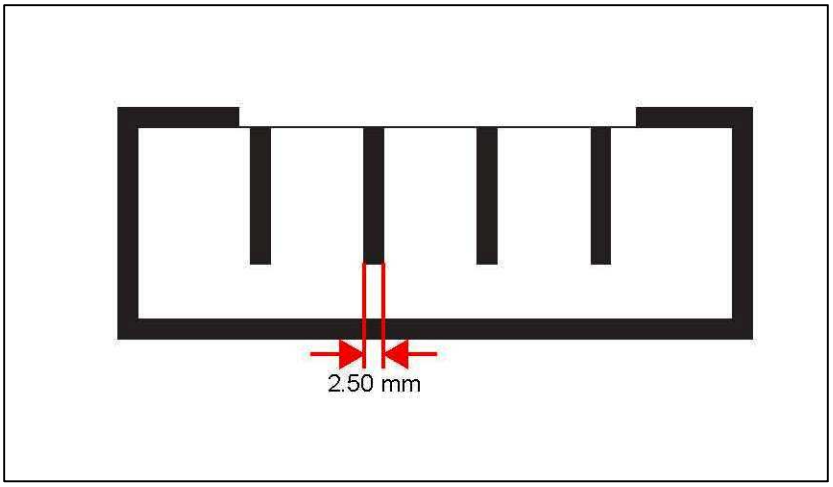

Figure 19: Second mask used to pattern gold electrodes. More space was created between each electrode to avoid contamination between electrodes, as well as electrical contact shorts.

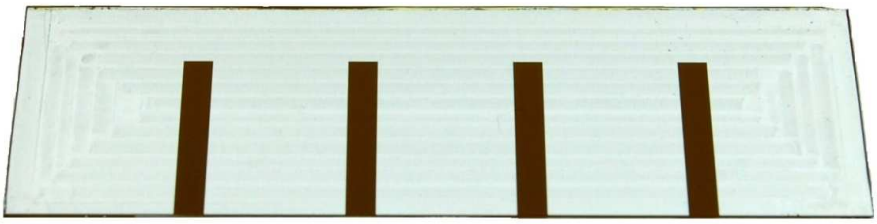

Figure 20: Standard 3”x1" glass slide patterned with the mask shown in Figure 19.

3.3.1.2 Counter and Reference Electrode Fabrication

To ensure functionality of our system, preliminary tests were completed using a platinum wire as the counter electrode, and a silver wire, with a coating of silver-chloride, as the reference electrode. We also fabricated reference and counter electrodes using conductive inks from Conductive Compounds Inc. The ink based carbon counter and silver-silver chloride reference electrodes were fabricated on a substrate of Melinex® 329, a non-pretreated polyester film from DuPont Teijin Films™. The Ag|AgCl ink (AGCL 675) was applied to the Melinex

substrate using an ink roller, and it was immediately cured at 140°C for 8 min. A strip of acid free double-sided adhesive was placed onto the opposite side of the Melinex before the electrodes were punched using a standard rectangular scrapbooking punch.

The counter electrodes were fabricated using Carbon ink (HTC-350) following the procedure above, but instead they were cured for 5 min at 140° C.

3.3.2 Electrochemical Cell Fabrication

In order to immobilize DNA strands onto the gold electrodes, a 15-20 µL droplet of the DNA solution had to be placed onto the electrode and allowed to incubate for 16-20 hrs in a box with 100% relative humidity. Once incubation was complete, another solution, the redox indicator, had to be applied and held in contact with the 3-electrode system during testing. In order to accomplish these tasks, a test platform was developed using two materials: poly(methyl methacrylate) or PMMA, and polydimethylsiloxane or PDMS. PMMA is a polymer used in numerous applications, often replacing glass; it is most commonly know as Plexiglas®. PDMS is a silicon-based organic polymer and, in this work, was mixed with a ratio of 10:1 (dimethylchlorosilane : polymerizer).

We created a test platform consisting of two PMMA plates which were pressed together by tightening six screws, as shown in Figure 21. The bottom plate, which contains a rectangular groove where the working electrode slide is placed and held flush with the bottom plate's surface, is shown in Figure 22.

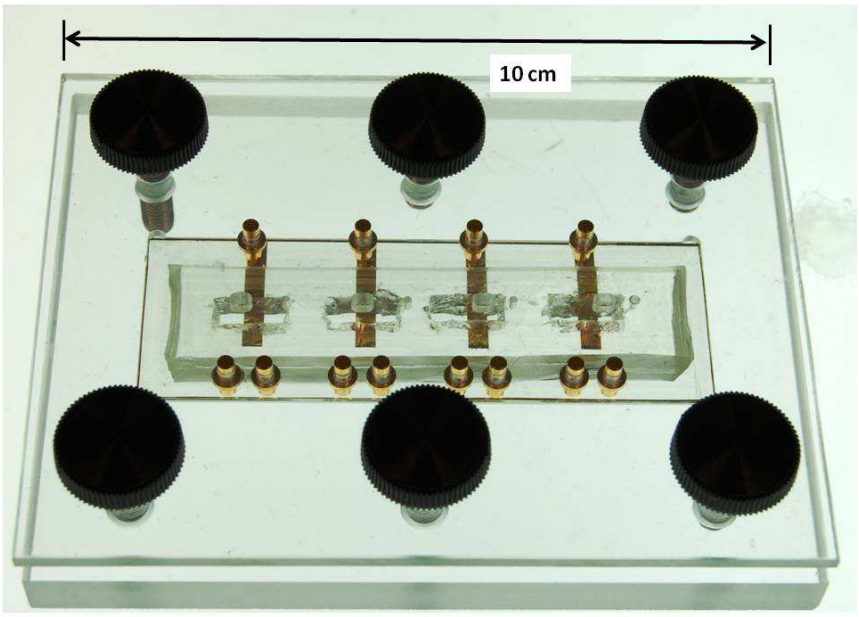

Figure 21: Electrochemical test platform containing working electrode slide. Six screws were used to press the two plates together, sandwiching a piece of PDMS in between, forming a seal between itself and the glass slide.

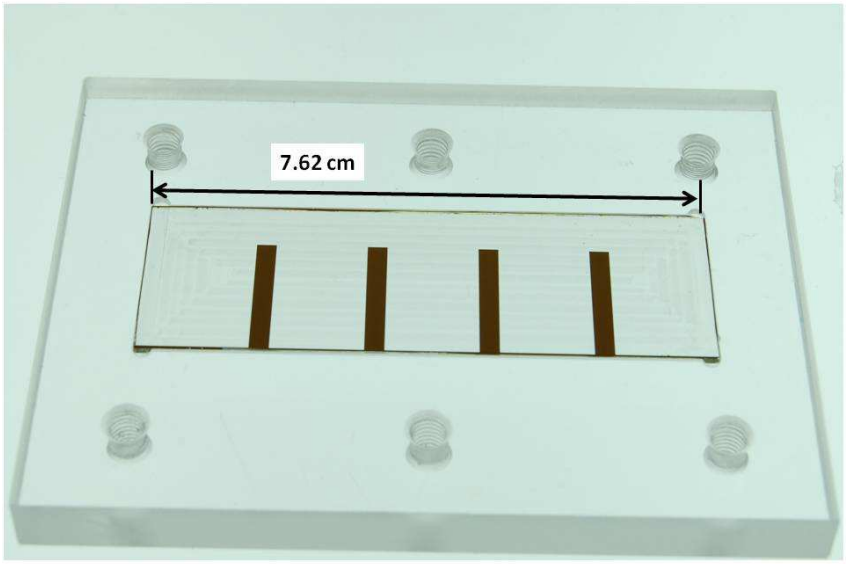

Figure 22: Bottom plate of electrochemical test platform. It contains a rectangular groove such that the working electrode slide sits flush with the PMMA surface.

A removable layer of PDMS, containing four inscribed rectangular chambers, was placed on top. As the plates were pressed together, a seal was formed between the glass and PDMS. The enclosed chambers were accessed by pipette through the holes in the top plate. Once incubation was complete and the top plate and PDMS were removed, the CE and RE were placed onto the slide, and a second PDMS piece was used to enclose each set of three electrodes, producing four test platforms. The gold-finished, spring-loaded pins that passed through the top plate established electrical contact to each electrode for electrochemical analysis. The functionality of the electrochemical cell was verified by using the benchtop potentiostat to perform cyclic voltammetry on both the standard and the miniaturized electrochemical cells, and comparing results. The tests were performed on bare gold in a solution of potassium ferricyanide. The test platform and results are shown below in Figure 23 and Figure 24, respectively.

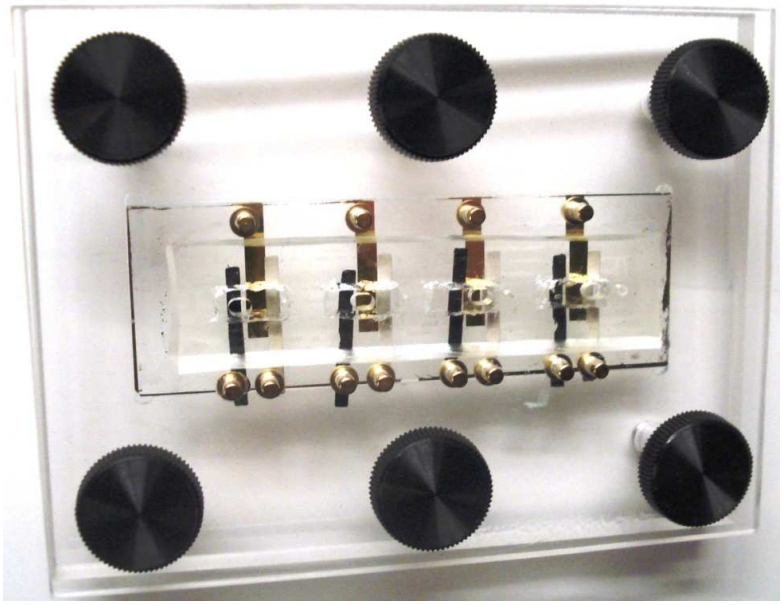

Figure 23: Electrochemical cell with ink based carbon and silver-silver chloride electrodes on a glass slide with patterned gold electrodes.

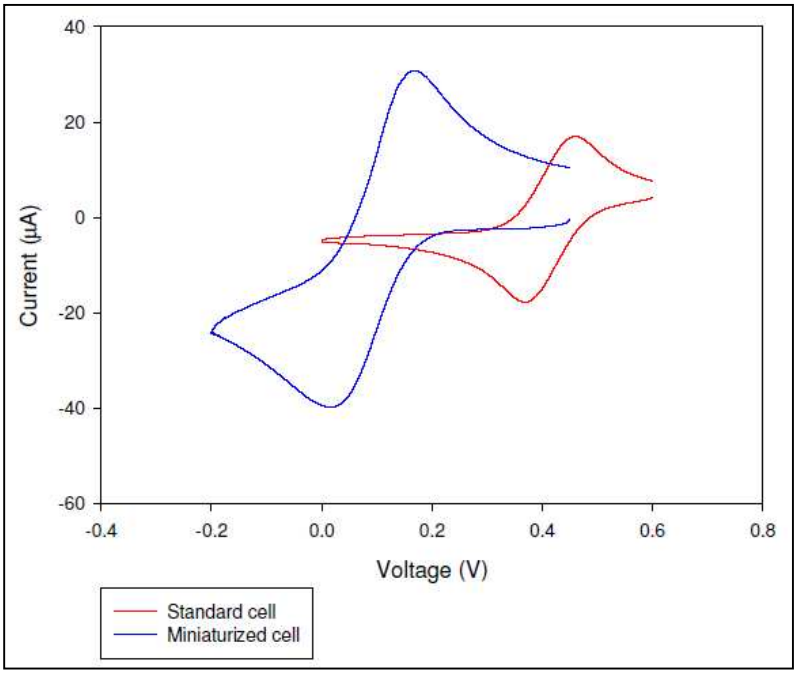

Figure 24: Electrochemical cell comparison – CV curves of 1 mM $K_3Fe(CN)_6$ in 100 mM NaCl on a gold electrodz. The differences in magnitude and DC shift were caused by the properties of the working and reference electrodes.

The area of the WE in the miniaturized cell was 1.89 times that of the WE in the standard cell; this difference in area caused the difference in magnitude of the two cyclic voltammograms. The DC shift was caused by a difference in the reference electrode potential. The results show that the miniaturized cell is performing correctly, and that calibration will be required if the results of the two systems are to be identical.

3.3.3 Process Improvements

Once the functionality of the cell and electrodes were verified, we improved the system. First, because the goal of this work is to eventually use screen printed microelectrodes, we decreased the area of each working electrode from 20 mm^2 to 9 mm^2. We also increased the number of electrodes per slide from four to sixteen, thus making efficient use of materials. Second, because the glass is hydrophilic, and visibly more hydrophilic than the gold, we suspected that the DNA was possibly being drawn towards the PDMS while being injected into the chambers. A removable layer of polytetrafluoroethylene (PTFE) or Teflon®, with inscribed chambers, was produced to ensure the DNA would not adhere to any surface but the gold; because Teflon® is hydrophobic, the DNA residing in a water based solution has no way to come into direct contact with the chamber walls. The improved mask is shown in Figure 25.

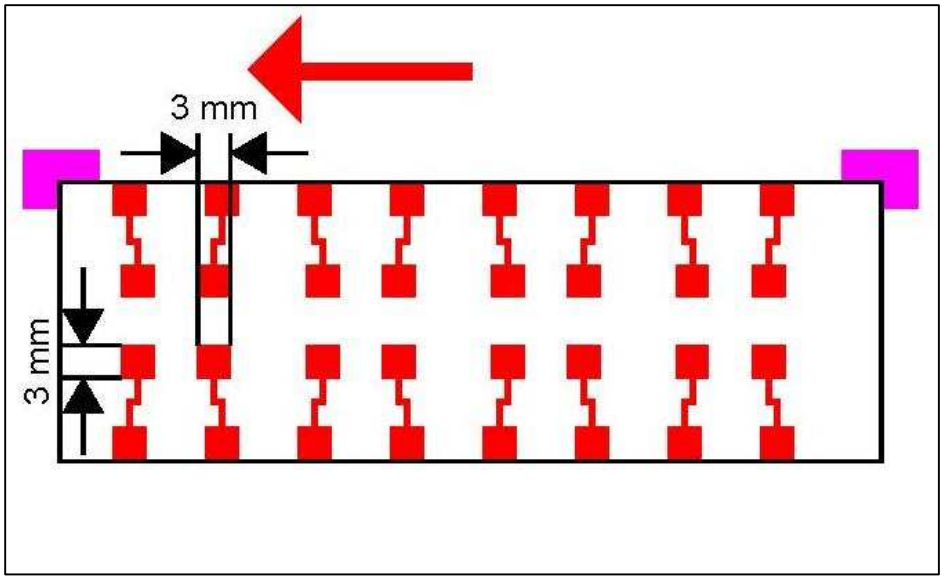

Figure 25: Improved mask used to pattern 16 working electrodes per slide, each electrode's working area is 9mm^2.

In order to accommodate the new WE slide pattern, the top plate of the test platform had to be re-designed. The final electrochemical cell is shown in Figure 26. Some of the chambers were filled with coloured water to test the Teflon to glass seal.

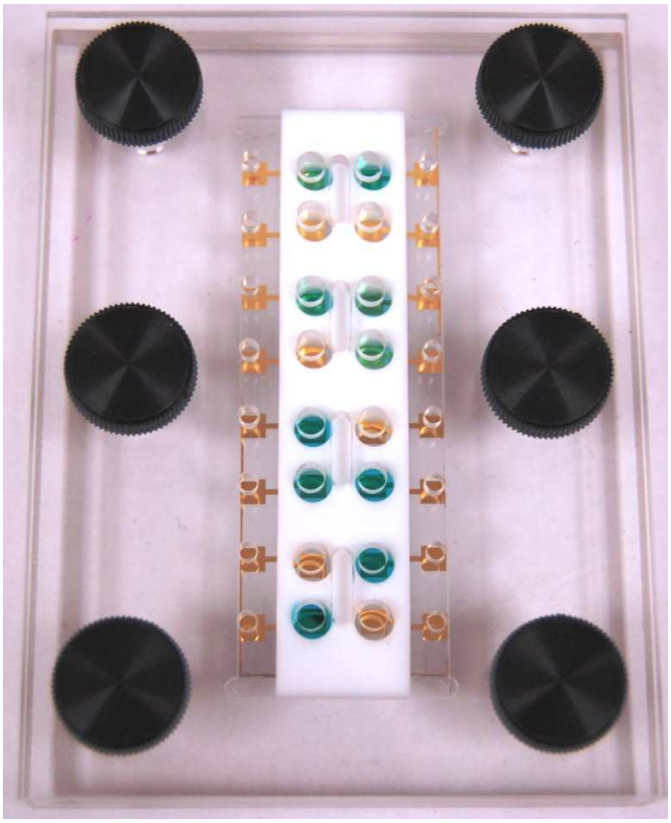

Figure 26: Final design of the electrochemical cell test platform. The Teflon chamber slide creates 16 possible test platforms over the working electrodes.

The goal of this design was to maximize the number of working electrodes per slide and hence the number of tests run with each slide preparation, therefore, the ink based electrodes were not taken into consideration of the design. To simplify the setup during this stage of testing, a silver wire (coated with silver chloride) and platinum wire were used as the RE and CE, respectively. The entire system setup is shown in Figure 27 and a magnified view of the electrode connections is shown in Figure 28.

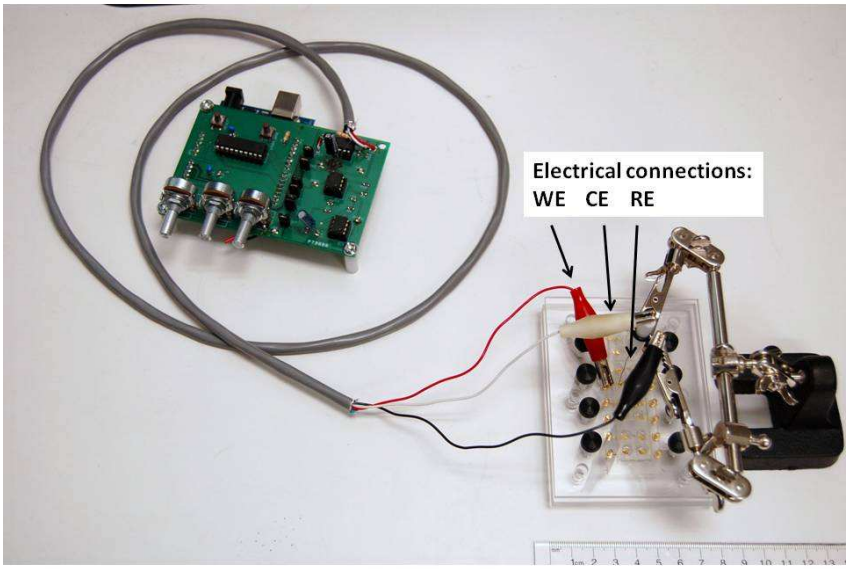

Figure 27: Final system setup including portable potentiostat and electrochemical cell.

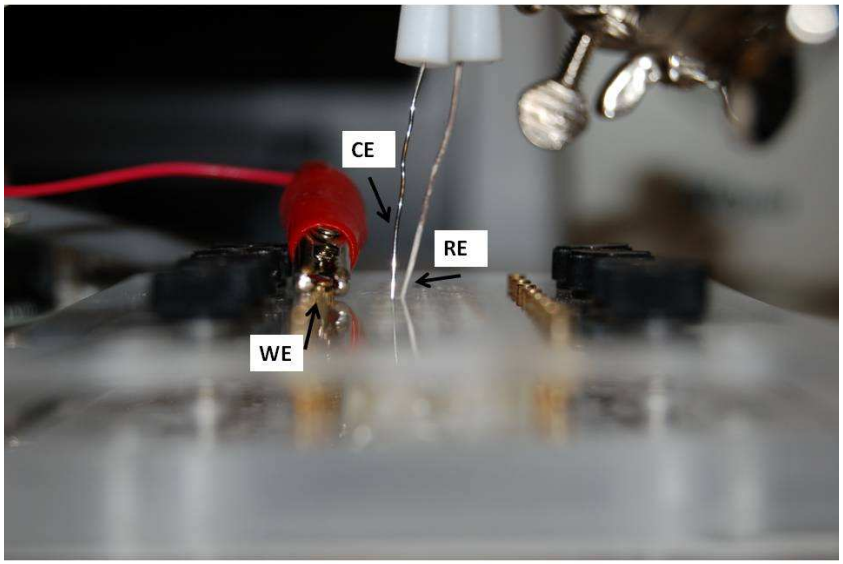

Figure 28: Magnified view of the electrode setup. The CE and RE are in contact with the solution through the access holes in the top plate of the cell.

4: DEVICE PERFORMANCE: PROTEIN DETECTION

The portable potentiostat system was designed to function as a protein detection biosensor alongside the electrochemical cell. To test the capabilities of our prototype, we performed lysozyme detection. As mentioned in chapter 2, lysozyme is a protein produced by the body which can be found within the blood. By demonstrating that the prototype can in fact detect this protein at a concentration of 0.5 µg/mL, we can presume any likewise protein detection could be accomplished. The following sections describe the procedure used to prepare the electrodes and run the detection tests and also present our results. For further details on the solutions recipes and the test procedure, refer to Appendix D.

4.1 Experimental Setup

4.1.1 Materials

Several solutions were used to prepare the DNA for immobilization on the gold working electrodes and to create the necessary environment to perform cyclic voltammetry tests. Table 1 introduces all solutions used while the next section, 4.1.2, describes their applications. More detail can be found in Appendix D.

Table 1: Materials used for electrode preparation and lysozyme detection testing.

Name	Composition	Function
DNA aptamer	HO-(CH2)6-S-S-(CH2)6-O-5'-ATCTACGAATTCATCAGGGCTAAAGAGTGCAGAGTTACTTAG-3'	lysozyme aptamer
Tris	tris(hydroxymethyl)aminomethane	To prepare buffer solution
TCEP	tris(2-carboxyethyl)phosphine hydrochloride	To reduce the S-S bond in the DNA aptamer
Immobilization buffer	20 mM Tris-HCl/0.1 M NaCl/5 mM $MgCl_2$ at pH 7.4	Buffer used to enhance immobilization of lysozyme aptamer on gold surface
MCH	6-mercapto-1-hexanol	To passivate the surface once the lysozyme aptamer has been immobilized
Redox marker solution	5 uM $[Ru(NH_3)_6]Cl_3$	Redox labelling

4.1.2 Procedures

The following sections describe the preparation of the working electrodes for lysozyme detection and the procedures followed during testing. For further details, see Appendix D.

4.1.2.1 Working Electrode Preparation

Purified lysozyme aptamer was obtained from Integrated DNA Technologies (IDT®) with a sequence of HO-$(CH_2)_6$-S-S-$(CH_2)_6$-O-5'-aptamer-3'.

The HO-$(CH_2)_6$ section, or thiol modifier, is used to protect the S-S bond. The section following this disulfide bond acts as a spacer which provides space between the DNA aptamer and the surface to which the sulphur will be bonded. This additional space helps align the aptamer in the desired orientation. As mentioned in section 3.3.1.1, the linkage or bond between gold and sulphur is known to be strong, therefore, in order for the chain to bind to the gold, the sulphur-sulphur (S-S) link must be broken. This break is accomplished by mixing the DNA in a solution of 10 mM TCEP in 100 mM tris buffer, and incubating the mixture for 4-12 hrs. The TCEP must then be removed from the solution, which is accomplished by using a column (essentially a filter) that is placed into a collecting tube containing tris immobilizing buffer (or tris I-B); the DNA solution is inserted into the top of the column and pushed through by spinning the solution in a centrifuge. (See Appendix D for more detail). To ensure the structure does not contain any unpredicted configurations, the solution is heated to 80°C for 5 min and allowed to cool at room temperature for 1 hour. During this time, the DNA structure unfolds and straightens while being heated, and then refolds while cooling to form the required structure. The DNA is then placed onto the cleaned gold electrodes and allowed to incubate for 16-20 hrs, in a box with 100% relative humidity. A representation of the immobilized aptamer is shown below in Figure 29.

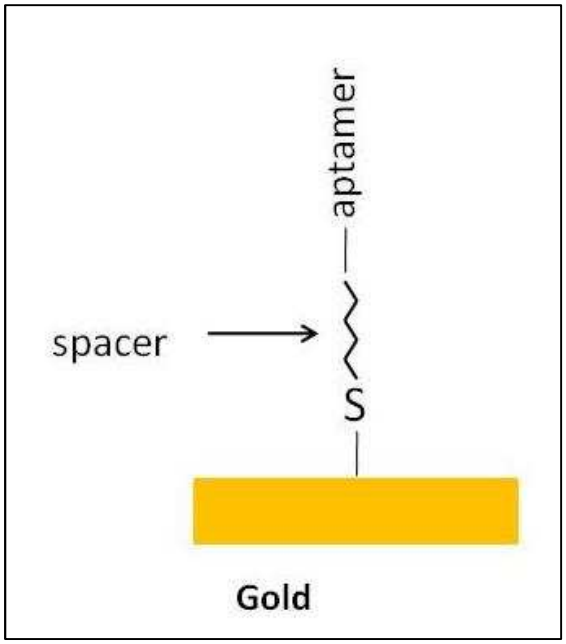

Figure 29: Lysozyme aptamer immobilized on gold after breaking the S-S bond.

However, we cannot presume that the gold was entirely covered. There may be areas where no DNA has bound, which will negatively affect the cyclic voltammetry tests. Therefore, MCH is placed onto each electrode and left for 1 hour: the MCH will fill in the gaps on the gold and bind wherever the DNA has not. Once the electrodes have been rinsed with 10mM tris buffer, they can be used for testing.

4.1.2.2 Cyclic Voltammetry Tests

Cyclic voltammetry tests were performed using the prepared lysozyme aptamer working electrodes described above; $[Ru(NH_3)_6]^{3+}$ (formed when ruthenium (III) hexamine chloride stock solution is added to tris buffer) was used as the redox marker, according to Cheng, Ge and Yu [15]. The detection of lysozyme was achieved by comparing the peak areas of the resulting cyclic

voltammograms before and after the presence of lysozyme within the system. To begin, the electrodes were exposed to the solution containing $[Ru(NH_3)_6]^{3+}$, which caused the cations to bind to the negatively charged phosphate backbone of the DNA. A cyclic voltammogram of this system was captured. The modified electrodes were then washed with tris buffer and incubated in a solution containing a selected concentration of lysozyme (between 0.5 ug/mL – 5 ug/mL). After incubation of 20 minutes, the positively charged lysozyme bounded to the DNA aptamer and reduced the net negative charge on DNA-modified surface. The $[Ru(NH_3)_6]^{3+}$ solution was once again added to the system; the scenario before and after lysozyme incubation is illustrated below in Figure 30. After lysozyme incubation, less $[Ru(NH_3)_6]^{3+}$ is able to bind to the DNA backbone, therefore weaker redox signals are expected. A substantial decrease in the peak area of the resulting cyclic voltammogram was observed. These results are discussed in the following sections.

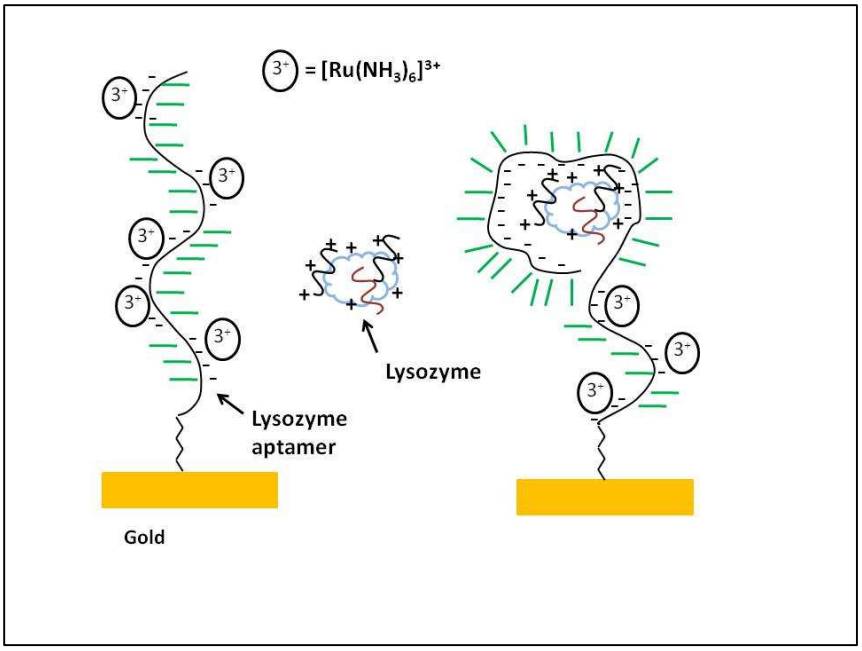

Figure 30: Graphic showing lysozyme aptamer immobilized on gold electrode, and demonstrating overall detection scheme [15].

4.1.3 Lysozyme Detection Test Results

Lysozyme detection tests were performed in both the standard cell as well as the miniaturized platform, the results of which are presented and discussed in the following two sections.

4.1.3.1 Standard Cell Test Results

Cyclic voltammetry tests were run at a scan rate of 500 mV/s on the standard cell using both the benchtop and portable potentiostat systems. Results were first obtained for the solution containing 5 μM $[Ru(NH_3)_6]Cl_3$. The cyclic voltammograms (CVs) are compared in Figure 31. Although both reduction peaks occur within 0.01 V of each other, the current read by the benchtop potentiostat changes much more quickly and peaks 0.51 μA lower than does the

current read by the portable potentiostat. At this stage, we cannot explain the difference in peak shapes. It seems that at a scan rate of 500 mV/s there may be a capacitive charge building up in the portable potentiostat circuit that is not capable of discharging quickly enough to follow the current change. This issue will require further investigation and is documented in chapter 5.

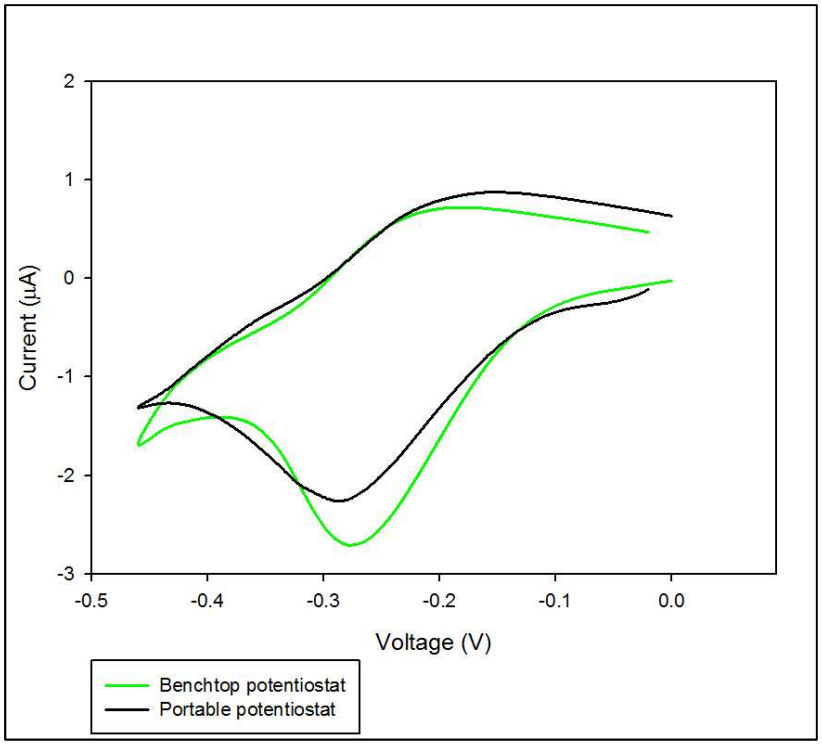

Figure 31: CVs of 5 uM $[Ru(NH_3)_6]^{3+}$ on lysozyme aptamer modified gold electrode, obtained from both the benchtop and portable potentiostat systems, respectively. The scan rate was 500 mV/s in both cases.

The WE was removed from the cell and rinsed three times with 10 mM tris buffer. Once the electrode was dried with nitrogen gas, a 15 µL droplet of 1 µg/mL lysozyme was applied to the electrode's surface and left for 1 hr. The electrode was again rinsed with tris, then covered with tris for 15 minutes. After being dried, the WE was a placed back into the cell. 1 mL of 10mM tris buffer

and 5 µL of 1 mM ruthenium was injected into the cell and allowed to incubate for 10 minutes prior to electrochemical detection. Cyclic voltammograms were captured using both systems. This entire process was repeated with a lysozyme concentration of 5 µg/mL. The results are shown in Figure 32 and Figure 33.

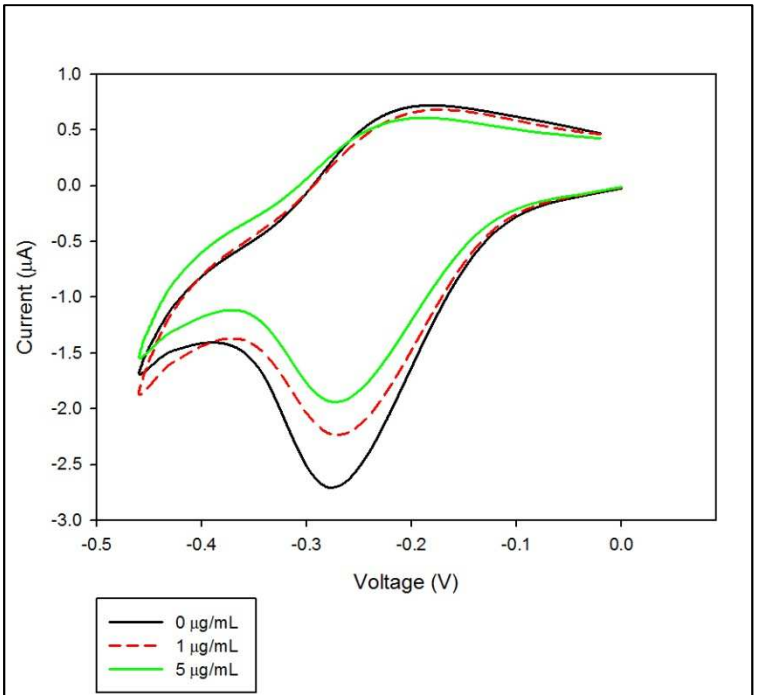

Figure 32: CVs of 5 µM $[Ru(NH_3)_6]^{3+}$ on lysozyme aptamer modified gold electrodes captured using a benchtop potentiostat at a scan rate of 500 mV/s.

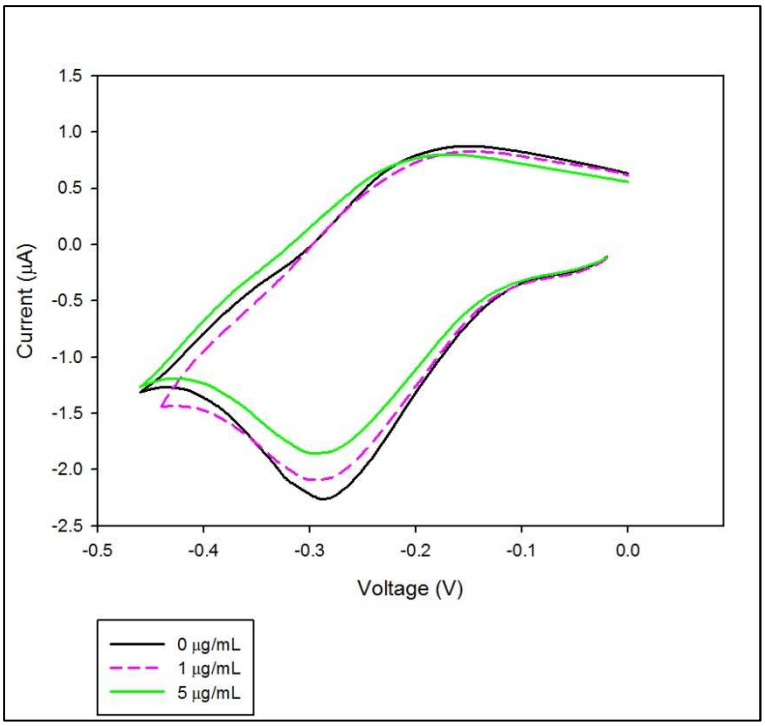

Figure 33: CVs of 5 µM $[Ru(NH_3)_6]^{3+}$ on lysozyme aptamer modified gold electrodes captured using the portable potentiostat at a scan rate of 500 mV/s.

The quantity of charge consumed during the reduction reaction is proportional to the area under the cathodic peak. By integrating the area under the cathodic peak, before and after the introduction of lysozyme, we should see a change indicating a decrease in charge exchanged, as shown below in Figure 34.

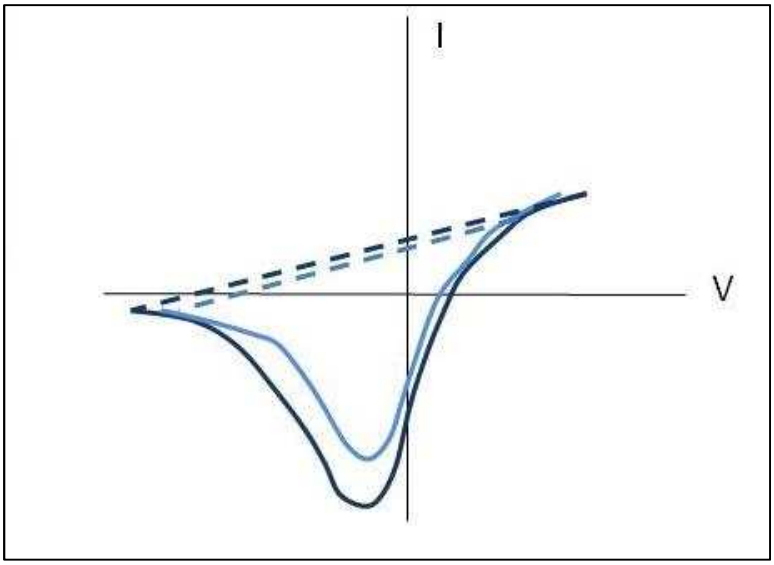

Figure 34: Decrease in cathodic peak before and after lysozyme was introduced into the system.

The change in charge was calculated using

$$\Delta Q = Q_i - Q_x, \tag{11}$$

where $Q_i$is the initial charge consumed calculated before the addition of lysozyme, and $Q_x$is the charge consumed calculated for lysozyme at a concentration of x. The concentration dependence of lysozyme calculated for both the benchtop and portable potentiostat systems are compared below in Figure 35.

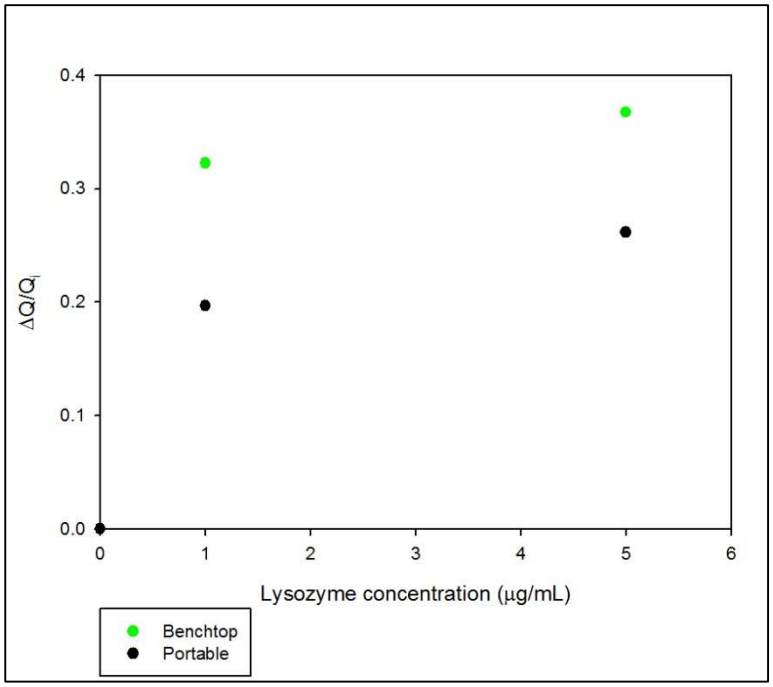

Figure 35: Concentration dependence of lysozyme on lysozyme aptamer modified gold electrodes in the standard cell.

The portable potentiostat is measuring a change in current and hence detecting the lysozyme, but the changes in current captured by the benchtop system are greater. This is due to the difference in peak shape and will need to be investigated further.

4.1.3.2 Miniaturized Cell Results

Lysozyme detection was then performed on the miniaturized cell, using a glass slide containing sixteen working electrodes. The same procedure described in section 4.1.3.1 was followed, however, a scan rate of 100 mV/s was used. This rate was found to be the optimal scan rate because the CVs produced from both potentiostat systems were comparable; the portable potentiostat captured the same rate of change of the current as did the benchtop system. The results are shown in Figure 36 and Figure 37. Because the results obtained at a scan rate of

500 mV/s had a magnitude 3.5 times that of the results obtained at 100 mV/s, the results are graphed on different scales in the y-axis; on the same scale, it is difficult to examine the changes in current at the 100 mV/s scan rate.

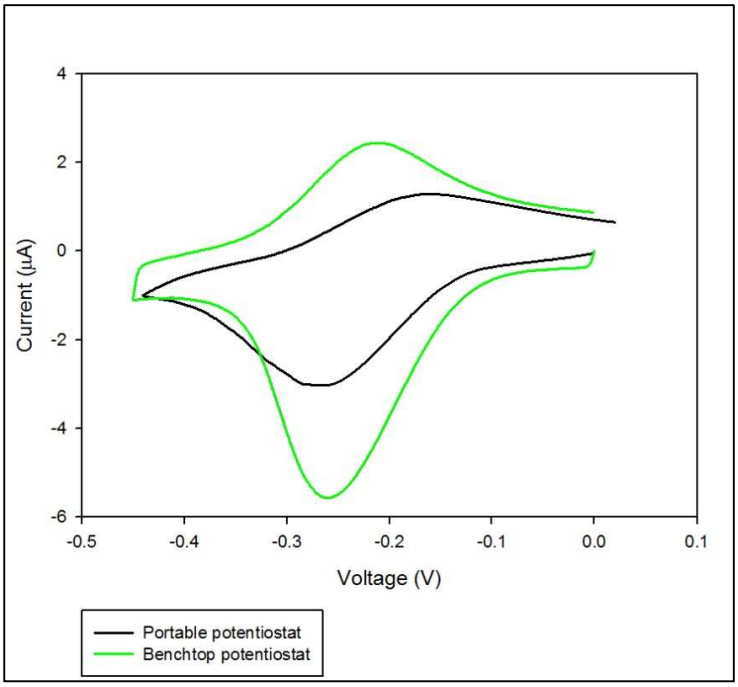

Figure 36: CVs of 5 uM $[Ru(NH_3)_6]^{3+}$ on lysozyme aptamer modified gold electrodes, obtained from both the benchtop and portable potentiostat systems, at 500 mV/s, before the addition of lysozyme.

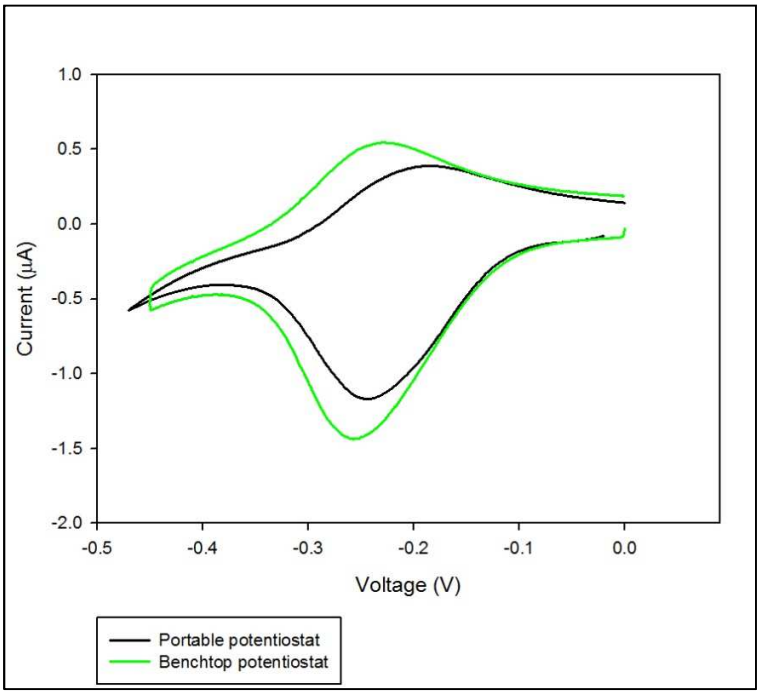

Figure 37: CVs of 5 uM $[Ru(NH_3)_6]^{3+}$ on lysozyme aptamer modified gold electrodes at 100 mV/s, before the addition of lysozyme.

Lysozyme concentrations ranging from 0.5 µg/mL – 5 µg/mL were used for perform electrochemical detection tests. The CVs generated by both potentiostat systems before the addition of lysozyme are compared in Figure 38. The reduction peaks of each graph occur at a voltage that differs by only 0.01 V, but the magnitude of the current read by the portable potentiostat at $E_{p(c)}$ is -0.5788 µA, 1.93 times the current read by the benchtop system. Because the purpose of this work was to develop a device that could detect protein markers, this issue in current difference is out of the scope of this work. However, if required, the portable system could be calibrated to produce results in the same magnitude as the benchtop device.

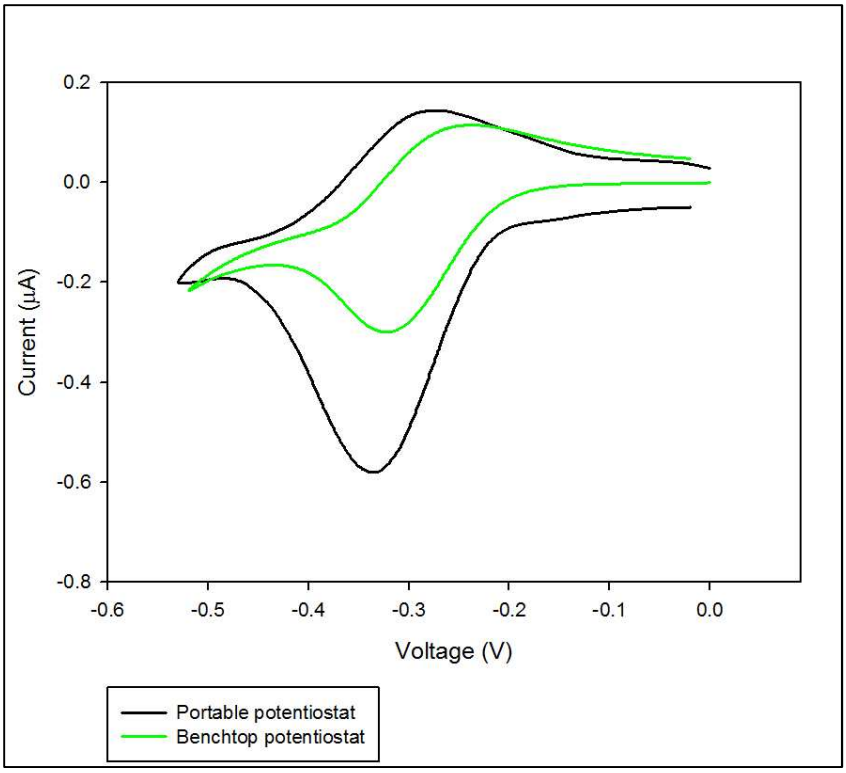

Figure 38: CVs for 5 µM $[Ru(NH_3)_6]^{3+}$ on lysozyme aptamer modified gold electrodes obtained from both benchtop and portable potentiostats at 100 mV/s.

A concentration of 0.5 µg/mL of lysozyme was introduced into the system following the same procedure described in section 4.1.3.1. Figure 39 and Figure 40 show the results obtained using the benchtop and portable potentiostat systems, respectively. Figure 41 compares the results.

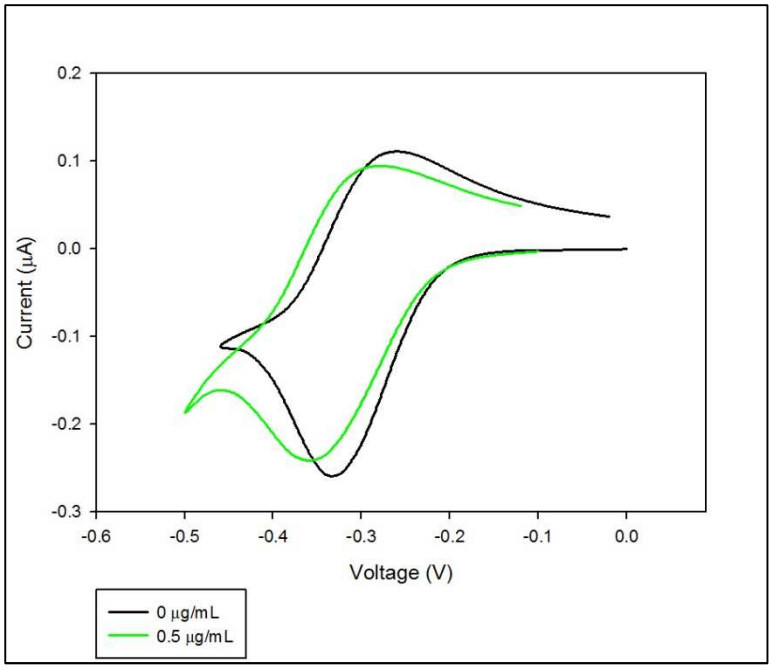

Figure 39: CV of 5 µM $[Ru(NH_3)_6]^{3+}$ on lysozyme aptamer modified gold electrode at 100 mV/s using benchtop potentiostat.

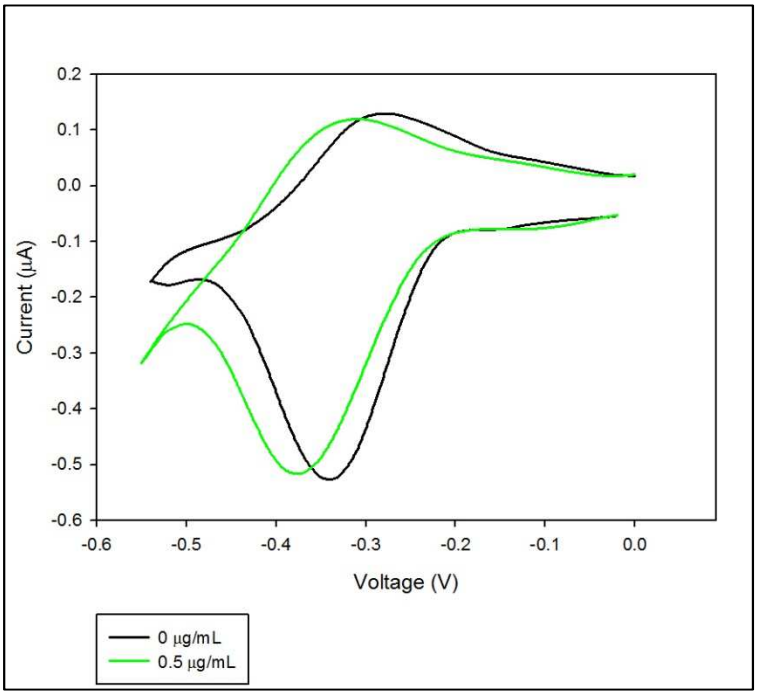

Figure 40: CV of 5 µM $[Ru(NH_3)_6]^{3+}$ on lysozyme aptamer modified gold electrode at 100 mV/s using portable potentiostat.

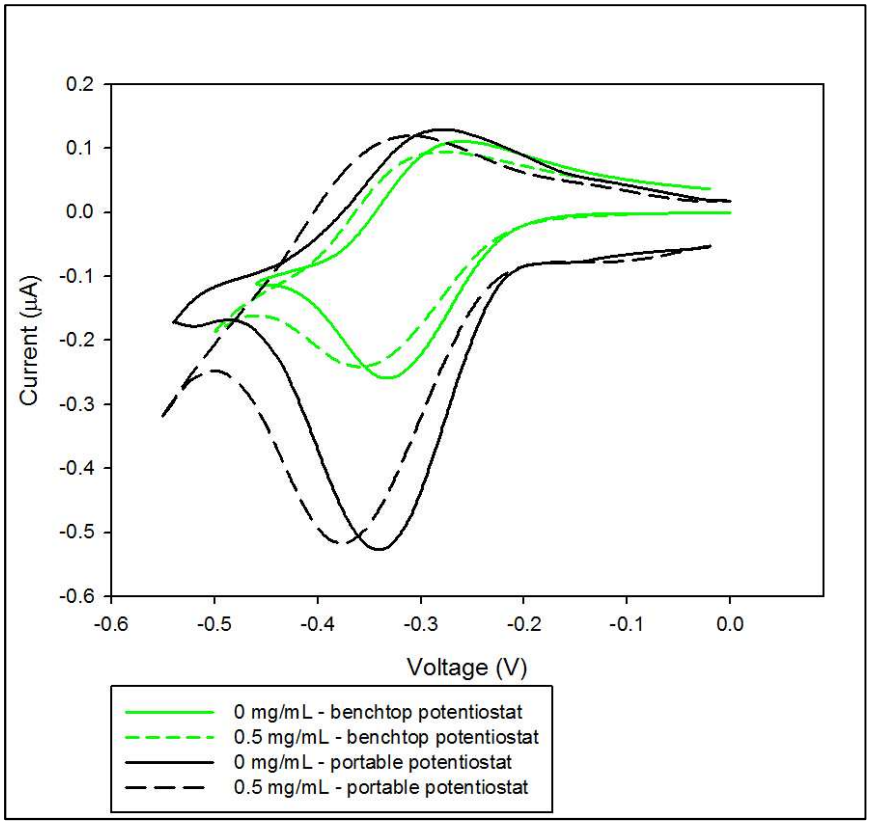

Figure 41: CVs of 5 µM $[Ru(NH_3)_6]^{3+}$ on lysozyme aptamer modified gold electrode captured using benchtop and portable potentiostats, respectively. Both results show a change in peak area with the addition of 0.5 µg/mL of lysozyme.

A change in the reduction peak area can been seen with the addition of 0.5 µg/mL of lysozyme, however, the magnitude of the results produced from the portable potentiostat are again higher in magnitude by 2.14 times than the results obtained from the benchtop system. Lysozyme concentrations of 2 µg/mL and 5 µg/mL were also tested. The results are shown in Figure 42. As the concentration of lysozyme increases, the change in current decreases.

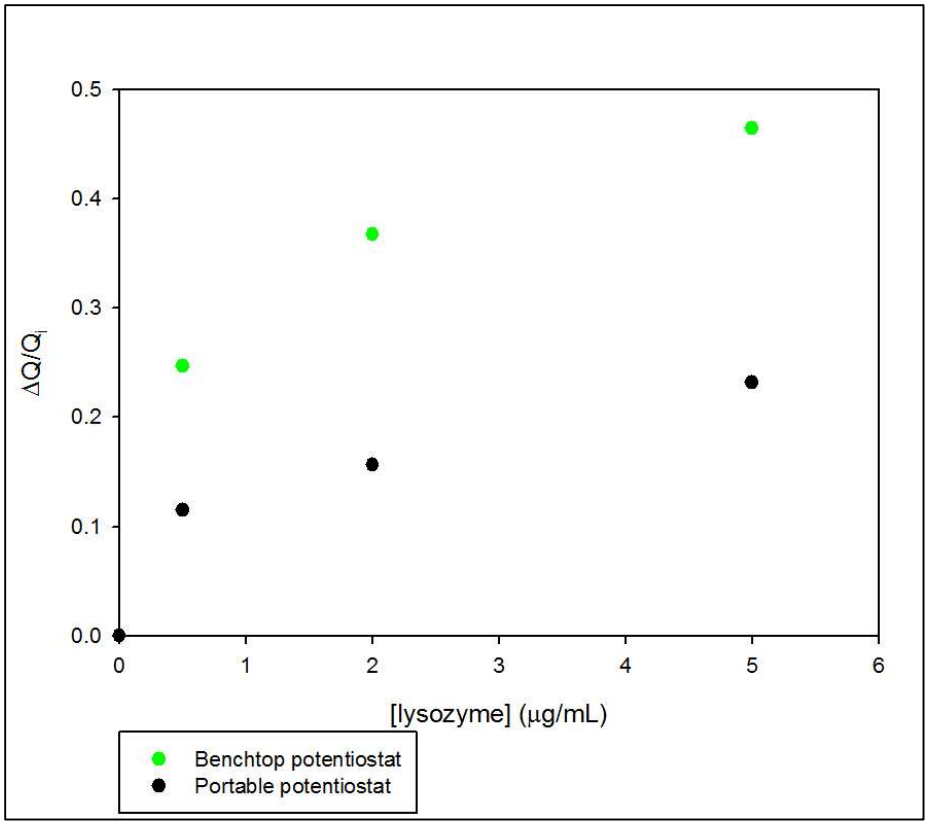

Figure 42: Concentration dependence of lysozyme on lysozyme aptamer modified gold electrodes.

Figure 42 shows that the benchtop potentiostat registered greater changes in charge transfer with the addition of lysozyme, than did the portable potentiostat. This is due to the difference in magnitude of the systems' respective CVs, an issue that will have to be addressed in future work. However, the portable potentiostat does register a change and therefore can detect lysozyme at a concentration of 0.5 μg/mL.

5: CONCLUSION AND FUTURE WORK

5.1 Future Work

In order for this project to continue and reach a more user friendly, dependable and, therefore, viable prototype, several changes are needed. First, the hardware must be redesigned to provide for an even higher resolution while allowing the user to select the voltage sweep range and scan rate. Increasing the number of data points above the current 50 points would provide for a smoother curve and result in fewer noise inflections. This increase in data points could be accomplished by using a 10 or 12 bit DAC and a digitally controlled attenuator, as well as a few software changes to accommodate the new parts. These changes would need to be implemented with the device size in mind as the hardware used to construct the circuit should be minimized; the next prototype should approach the size of other biosensors currently on the market.

In addition, the selection of initial and peak voltages as well as the scan rate would need to be reconfigured. Implementing these user controls into the software would result in fewer external switches, again minimizing device size. Second, the electrode system needs to be refined so that a screen printing process can be used such that all three electrodes could reside on a single disposable strip of polyester film. The electrode fabrication method would need to be configured alongside the chemistry process because the current method of DNA isolation would not be feasible for mass production. And third, a new

software interface as well as a data handling system needs to be created. An algorithm to calculate the area of the peaks of the resulting cyclic voltammograms in real time is required.

Once all these adjustments are made, protein detection repeatability and precision will need to be tested for. Overall, several adjustments and fixes must be addressed, but they are all viable and, therefore, present no major obstacle in bringing this device to a marketable prototype.

5.2 Contribution

In taking an interdisciplinary approach to this research, we have combined microelectronic design with advances in aptamer-based protein detection, and developed an innovative biosensor prototype. We have also developed a basis for the fabrication of the required electrode test platform, and we have determined which materials are ideal for aptamer-based protein detection. We have succeeded in showing that our prototype can detect lysozyme at a concentration of 0.5 ug/mL and is, therefore, comparable to current benchtop systems, except that our prototype was fabricated for less than one tenth of the cost of the benchtop system. This thesis provides the ground work for a marketable biosensor.

5.3 Conclusion

This thesis describes the fabrication and design of a biosensor prototype, developed to perform cyclic voltammetry for the purpose of protein detection and diagnostics. A working prototype was developed and tested for functionality using

lysozyme aptamer, and the results were compared to those obtained from a benchtop potentiostat.

Development of the biosensor prototype was a two part process consisting of the microelectronics design of the USB powered portable potentiostat, and the fabrication of the miniaturized electrochemical cell and electrode system. Four iterations of circuit designs were required before the output noise was reduced to below 100 pA. The final design was established once the number of op amp stages throughout the circuit were minimized, and the circuit was operating within a 0 V to 5 V range – the latter of which eliminated the signal manipulation required to convert the analog output into a digital signal. In addition to the circuit, the electrochemical cell also underwent three redesigns before reproducible cyclic voltammetry results could be obtained. Reproducibility was accomplished by creating working electrodes of definitive size and fabricating a platform that would provide for greater batches of testing without breaking the working electrodes during insertion and removal.

The end result was a working prototype of a USB powered biosensor alongside an electrochemical cell. While there are improvements to be made the work presented in this thesis forms a basis for the development of a marketable biosensor prototype.

APPENDICES

Appendix A – Equations and Calculations

Surface concentration

$$\Gamma = \frac{Q}{nFA}$$

To find the surface concentration of ruthenium in molecules/cm^2 on the working electrodes, we have:

$$\Gamma_{\mathrm{Ru}} = \frac{Q}{(1)(96485)(0.09)} = Q(1.152 \text{ x } 10^{-4}).$$

Surface Density

Using the surface concentration of ruthenium, we can then calculate the surface density of DNA using

$$\Gamma_{DNA} = \Gamma_{Ru}\left(\frac{z}{m}\right)$$

where *z* is the valence of the redox ion (for ruthenium, *z* = 3), and *m* is the number of nucleotides in the DNA (for the lysozyme aptamer *m* = 42). Therefore, the surface density of DNA, or the number of molecules per cm^2 is

$$\Gamma_{DNA} = \Gamma_{Ru}(0.0714) = Q(8.2286 \text{ x } 10^{-6})$$

The ideal surface density for lysozyme aptamer is 1.6 x 10^{12} – 1.8 x 10^{12} molecules/cm^2

Conditions for a Spontaneous Chemical Reaction

$$E > 0,$$

$$\Delta G^{\circ} = -nFE^{\circ} < 0,$$

where *E* is the half cell potential, *G* is the free-energy change and *F* is the Faraday constant.

Appendix B – Microcontroller Code

```
/****************************Final working program************************

This program is designed to control the counter and DAC to generate an adjustable triangular wave for one cycle.

The wave start from the highest then go down to the lowest point and go up again stopping at the highest point.

The lowest point, highest point and the rate are controled by three potentiometers

The output current, reference voltage and Vcc level are read from analogIn pins

*******************************************************************************/

//Digital Pin
int clk_pulse = 4;          //Clock pulse pin
int reset_counter = 8;      //master reset for counter
int ud_counter = 5;         //Up/Down pin for counter
int cs_counter = 6;         //chip selection for counter
int oe_counter = 7;         //output enable for counter
int dac_cs = 2;             //chip select for DAC
int dac_wr = 3;             //write for DAC
int start = 9;              //start counting

//Analog Pin
int startpin = 5;           //lowest value of wave
int peakpin = 4;            //higest value of wave
int timepin = 3;            //control the rate
int dataread = 2;           // data in for testing
int reference = 1;          //read the voltage at reference electrode
int vccpin = 0;             //read the voltage level of vcc
double virtualGround = 0;//set virtualGround to 0
int output = 0;             //DAC OUTPUT
int up_down = HIGH;         //LOW for down, HIGH for up;
int i = 0;                  //general counter
int start_value = 0;
```

```
int peak_value = 255;    //start the counter at highest count
long delayTime;          //variable assigned to convert an array to integer
double vcc = 0;          //initiate vcc to zero
double start_voltage = 0;//set start voltage to zero
double peak_voltage = 5;//set
double rate = 0;
double ref_voltage = 0;
double current = 0;

void clockGen(int port) { //generate one clock pulse
        digitalWrite(port, HIGH);
        delayMicroseconds(1);

        digitalWrite(port, LOW);
        delayMicroseconds(1);
}

//to transfer data into DAC and out (according to timing diagram)
void validDAC() {
        //enable DAC and latch date to input regiter
        digitalWrite(dac_cs, LOW);
        digitalWrite(dac_wr, LOW);
        delayMicroseconds(2);
        digitalWrite(dac_wr, HIGH);
        digitalWrite(dac_cs, HIGH);
        delayMicroseconds(1);
}

void showParameter(){

        int old_delayTime;
        int old_start_value;
        int old_peak_value;
        setParameter();              //Read the parameter value from analogIn once
        vcc = analogRead(vccpin);//Read the Vcc
        vcc = 2127.84/(1023-vcc); //calculate the real vcc:  (Vcc-Vzener)/Vcc =
                                        analogRead/1023
```

```
        Serial.println("***********VCC,,,,");
        Serial.println(vcc, 5);
        while(digitalRead(start)==LOW){
                old_delayTime = delayTime;
                old_start_value = start_value;
                old_peak_value = peak_value;
                setParameter();//read the parameter again

                //if the new parameter and old one are different, display the parameter,
                otherwise read the parameter again until the start button is pressed

        if((old_delayTime!=int(delayTime))||(old_start_value!=int(start_value))||(old_peak
        _value!=int(peak_value))){
                        start_voltage = (vcc*double(start_value))/255;
                        peak_voltage = (vcc*double(peak_value))/255;

                        //voltage for one step = vcc/255.delayTime is the time for one
                        step *1000000 is to change V/ms to mV/s
                        rate = (vcc*1000000/255)/double(delayTime);

                         Serial.print("DATA,,,,");
                        Serial.print(",S_a:,");
                        Serial.print(start_voltage-vcc/2);
                        Serial.print(",P_a:,");
                        Serial.print(peak_voltage-vcc/2);
                        Serial.print(", R :,");
                        Serial.print(rate);
                         Serial.print(",mv/s,");
                        Serial.println(",CR");
            }
        }
        while(digitalRead(start)==HIGH);
}
//to set the parameters.
void setParameter(){
delayTime = analogRead(timepin);
```

```
        /*the rate is required from 10mv/s to 100mv/s,so the delay time calculated is from
        1882ms to 188ms.the calculation is change the delay time read from analog in
        which is from 0 to 1023 to the range from 188 to 1882*/


delayTime = int(delayTime*1844.4/1023)+37.6;
start_value = analogRead(startpin);
peak_value = analogRead(peakpin);
start_value =int((start_value)/4);
peak_value =int((peak_value)/4)-1;
}


        //sample 9 times per step and find the average of the value
void findAverage(){
double ref_ave=0;
 double current_ave =0;
ref_ave = analogRead(reference);
current_ave = analogRead(dataread);


        for(i=0;i<8;i++){
                delay(delayTime/8);
                ref_voltage = analogRead(reference);
                current = analogRead(dataread);
                ref_ave = (ref_ave + ref_voltage)/2;
                current_ave = (current_ave + current)/2;
                }
                ref_ave = -1*(ref_ave*vcc/1023 - vcc/2);
                current_ave = (current_ave*vcc/1023 - vcc/2)*6.73;//1.0132;
                //Read in voltage from converter, divide by 10k/100k or whatever to get
                current, x10^6 for uA
                Serial.print("DATA,,");
                Serial.print(ref_ave);
                Serial.print(",");
                Serial.print(current_ave, 4);
                 Serial.println(",CR");
}


void setup() {
        //to set directions of pins of Arduino
```

```
pinMode(clk_pulse, OUTPUT);
pinMode(reset_counter, OUTPUT);
pinMode(ud_counter, OUTPUT);
pinMode(cs_counter, OUTPUT);
pinMode(oe_counter,OUTPUT);
pinMode(start,INPUT);
pinMode(dac_cs, OUTPUT);
pinMode(dac_wr, OUTPUT);
digitalWrite(dac_cs, HIGH);
digitalWrite(dac_wr, HIGH);

//initialize the counter
digitalWrite(cs_counter,HIGH);//disable counter
digitalWrite(reset_counter,HIGH);
digitalWrite(oe_counter,HIGH);
Serial.begin(9600);
showParameter();
digitalWrite(reset_counter, HIGH);
delayMicroseconds(100);
digitalWrite(reset_counter, LOW);
delayMicroseconds(100);
digitalWrite(reset_counter, HIGH);
delayMicroseconds(100);

//Clock in Gain and Buffer Values for DAC
digitalWrite(dac_cs, LOW);
delayMicroseconds(10);
digitalWrite(dac_wr, LOW);
delayMicroseconds(10);

digitalWrite(dac_cs, LOW);
delayMicroseconds(10);
digitalWrite(dac_wr, LOW);
delayMicroseconds(10);
digitalWrite(ud_counter, up_down);//set the counter for count up or down
digitalWrite(cs_counter,LOW);//enable the counter
delayMicroseconds(100);
```

```
}

void loop() {

  /*if the counter is counting down,
   check if the output is 0 or not,
   if so, change the counter to count up

   if the counter is counting up,
   check if the output is 255 or not,
   if so, change the counter to count down
   */

//count up to the peak value without showing output at the counter output

      while(output<peak_value){
          clockGen(clk_pulse);
          output++;
          }

          digitalWrite(oe_counter,LOW);   //enable counter output
          validDAC();                     //enable DAC
          delay(25000);                   //delay 5 seconds to stabelize
          up_down = LOW;                          //let counter count down first
          digitalWrite(ud_counter,up_down);
          while(1){

                    if (up_down == LOW) {
                    if (output == start_value) {
                              up_down = HIGH;
                              digitalWrite(ud_counter, up_down);
                              clockGen(clk_pulse);
                              output++;
                    }
                    else {
                              clockGen(clk_pulse);
                              output--;
```

```
                }
                }
                else {
                if (output == peak_value) {
                        up_down = LOW;
                        digitalWrite(ud_counter, up_down);
                        clockGen(clk_pulse);
                        output--;
                        break;   //stop counter after one cycle
                }
                else {
                        clockGen(clk_pulse);
                        output++;
                }
                }
        validDAC();//convert the counter output to analog signal.
        findAverage();//sample the data and find the average
        virtualGround = analogRead(analogTestPin);
        }
        while(1);
}
```

Appendix C – Microfabrication Recipes

Electrode Fabrication Recipe

1. Start with an emf Inc pre-coated, 3”x1”, 10/90 nm chrome/gold glass slide
2. Spin on Shipley 1813 at 3000rpm for 30 seconds
3. Softbake at 100°C for 15 minutes
4. Expose with mask for 40 seconds
5. Develop in MF-319 for 60 seconds
6. Rinse in DI water for 3 minutes
7. Etch Au in Au etchant for 60 seconds
8. Rinse in DI water for 3 minutes
9. Etch Cr in Cr etchant for 20 seconds
10. Expose WITHOUT MASK for 40 seconds
11. Develop in MF-319 for 60 seconds to remove photoresist

RCA SC-1 Clean (Organics) Recipe

1. Heat 1000mL of DI water to 70°C
2. Add 200mL 30% ammonium hydroxide (NH_4OH)
3. Add 200mL 50% hydrogen peroxide (H_2O_2)
4. Stabilize temperature at 80 $\pm$ 5 °C
5. Insert slides and leave for 10 minutes
6. Remove slides and rinse for 3 minutes in running DI water

Appendix D – Chemistry Recipes and Procedures

Chemical Recipes

10x Tris buffer stock

12.114 g tris(hydroxymethyl)aminomethane (Tris base) (100 mM)
1 L Millipore purified water

Add Tris to 500 mL Millipore water. Adjust pH to 7.4 with HCl. Add water to 1 L volume.

10 mM tris(2-carboxyethyl)phosphine (TCEP) solution

0.00287 g tris(2-carboxyethyl)phosphine hydrochloride
1 mL 10x Tris buffer stock (100 mM Tris)

Keep in -20^{o}C. Remake once every few months.

1 mM ruthenium (III) hexamine chloride stock solution

0.0031 g ruthenium (III) hexamine chloride (as accurate as possible)
10 mL Millipore purified water

Ruthenium (III) hexamine chloride is light sensitive and not stable in solution. This stock must be remade once every few months

Add ruthenium (III) hexamine chloride to water in the dark. Divide into 500 µL aliquots. Keep in -20^{o}C. Do not refreeze once thawed.

5 µM $[Ru(NH_3)_6]^{3+}$ electrochemical detection buffer

5 mL 10x Tris buffer stock (10 mM final)

44.75 mL Millipore water

250 µL 1 mM ruthenium stock

Add ruthenium stock solution in the dark. Keep in the dark and de-aerate with $Ar_{(g)}$ or $N_{2(g)}$ prior to use.

10x lysozyme binding buffer stock

10 mL 10x Tris buffer stock (20 mM final)

40 mL Millipore water

0.2922 g NaCl (100 mM final)

0.0508 g $MgCl_2*6H_2O$ (5 mM final)

100x 6-mercapto-1-hexanol (MCH) stock

14 µL 6-mercapto-1-hexanol (MCH damages pipettes, use caution)

1 mL 95% ethanol

Add MCH in fumehood. Keep in -20^{o}C.

1 mM MCH solution

10 µL 100x MCH stock

100 µL 10x Tris stock

890 µL Millipore water

Keep in -20^{o}C.

Working Electrode Preparation and Test Procedure

1. Mix 0.3 µL of 98.2 µM DNA in 35.7 µL 100 mM tris buffer with 4 µL 100 mM TCEP.

2. Spin down the solution, cover with foil and leave in a dark area for 4-12 hours.
3. Using a G-50 column, spin in centrifuge for 1 minute at 3000 rpm.
4. Remove from centrifuge, pour out excess buffer and add 200 µL tris I-B buffer. Spin again for 1 minute at 3000 rpm.
5. Repeat step 4 5 times.
6. Discard the collecting tube and get a fresh one. Put the 40 µL of DNA and TCEP solution into the column. Spin in centrifuge for 3 minutes at 3000 rpm.
7. Place the collecting tube containing the DNA onto a hot plate at 80°C for 5 minutes. Remove and allow to cool to room temperature for 1 hour.
8. Clean a pattern slide in Piranha (3:1 mixture of concentrated H_2SO_4 and 30% H_2O_2) at 90°C for 8 minutes.
9. Dry with nitrogen gas.
10. Put 10 µL of lysozyme aptamer onto each electrode. Incubate 16-20 hours.
11. Rinse three times with tris buffer.
12. Mix 2 µL 1 mM MCH in 10 mM tris buffer.
13. Rinse each electrode with MCH solution, then cover with MCH solution for 1 hour.
14. Rinse each electrode with tris buffer three times, then cover with tris buffer for 15 minutes.
15. Mix 1 mL of 10 mM tris with 5 µL 1 mM ruthenium solution.
16. Dry electrodes and place in electrochemical cell. Put 10 µL of ruthenium/tris solution into each chamber. Wait 10 minutes before running cyclic voltammetry tests.
17. Rinse electrodes three times with tris buffer. Dry electrodes.
18. Apply lysozyme and leave 1 hour.
19. Repeat steps 14-17 for additional concentrations of lysozyme.

Reference List

[1] Unknown, "Canaries Dwarfted," *Economist*, vol. 320, pp. 96-97, 1991.

[2] C. D. Association, "The prevalence and costs of diabetes," 2009.

[3] M. Famulok, "Bringing picomolar protein detection into proximity," *Nature Biotechnol*, vol. 20, pp. 448, 2002.

[4] Y. Shi, H. Dou, A. Zhou, and Y. Chen, "Design and fabrication of a miniaturized electrochemical instrument and its preliminary evaluation," *Sensors and Actuators B: Chemical*, vol. 131, pp. 516-524, 2008.

[5] J. R. Blanco, F. J. Ferrero, J. C. Campo, J. C. Anton, J. M. Pingarron, A. J. Reviejo, and J. Manso, "Design of a Low-Cost Portable Potentiostat for Amperometric Biosensors," *IEEE conferences*, pp. 690-694, 2006.

[6] M. D. Steinberg and C. R. Lowe, "A micropower amperometric potentiostat," *Sensors and Actuators B: Chemical*, vol. 97, pp. 248-289, 2004.

[7] E. M. Avdikos, M. I. Prodromidis, and C. E. Efstathiou, "Construction and analytical applications of a palm-sized microcontroller-based amperometric analyzer," *Sensors and Actuators B: Chemical*, vol. 107, pp. 372-378, 2005.

[8] D. C. Harris, "Quantitative Chemical Analysis," pp. 270-320, 348-372, 2007.

[9] J. Wang, "Analytical Chemistry," pp. 29-42, 67-85, 115-136, 165-185, 2006.

[10] M. Javanmard, A. H. Talasaz, M. Nemat-Gorgani, F. Pease, M. Ronaghi, and R. W. Davis, "Electrical detection of protein biomarkers using bioactivated microfluidic channels," *National Institutes of Health*, vol. 9, pp. 1429-1434, 2009.

[11] K. J. Odenthal and J. J. Gooding, "An introduction to electrochemical DNA biosensors," *The Analyst*, vol. 132, pp. 603-610, 2007.

[12] R. W. Cattrall, "Chemical Sensors," pp. 1-3, 30-36, 1997.

[13] D. Wild, "The immunoassay Handbook," 201.

[14] S. Wolfl and S. Diekmann, "Aptamers," *Reviews in Molecular Biotechnology*, vol. 74, pp. 3-4, 2000.

[15] A. K. H. Cheng, B. Ge, and H.-Z. Yu, "Aptamer-Based Biosensors for Label-Free Voltammetric Detection of Lysozyme," *Analytical Chemistry*, vol. 79, pp. 5158-5164, 2007.

[16] G. Link, "Smart Designed Aptamers: Applications & Effective Design Options."

[17] E. J. Cho, J.-W. Lee, and A. D. Ellington, "Applications of Aptamers as Sensors," *Annual Review of Analytical Chemistry*, vol. 2, pp. 241-264, 2009.

[18] A. V. Gopinath and D. Russell, "An inexpensive Field-Portable Programmable Potentiostat," *Chem. Educator*, vol. 11, pp. 23-28, 2006.

[19] http://www.parallax.com/tabid/393/Default.aspx [June 14, 2010].

[20] J. C. Love, L. A. Estroff, J. K. Kriebel, R. G. Nuzzo, and G. M. Whitesides, "Self-Assembled Monolayers of Thiolates on Metals as a Form of Nanotechnology," *Chem. Rev.*, vol. 105, pp. 1103-1169, 2005.
[21] C. Vericat, M. E. Vela, G. A. Benitez, J. A. Martin Gago, X. Torrelles, and R. C. Salvarezza, "Surface characterization of sulfur and alkanethiol self-assembled monolayers on Au(111)," *Journal of Physics: Condensed Matter*, vol. 18, pp. R867-R900, 2006.